

## Distribution Agreement

In presenting this thesis or dissertation as a partial fulfillment of the requirements for an advanced degree from Emory University, I hereby grant to Emory University and its agents the non-exclusive license to archive, make accessible, and display my thesis or dissertation in whole or in part in all forms of media, now or hereafter known, including display on the world wide web. I understand that I may select some access restrictions as part of the online submission of this thesis or dissertation. I retain all ownership rights to the copyright of the thesis or dissertation. I also retain the right to use in future works (such as articles or books) all or part of this thesis or dissertation.

Signature:

Yaxi Du

---

4/3/2024

---

Date

Decoding the Hidden Mechanisms of Soil Carbon Cycle in Response to Climate Change

By

Yaxi Du

Master of Science

Environmental Science

Debjani Sihi, PhD  
Advisor

Shaunna Donaher, PhD  
Committee Member

Jacqueline Mohan, PhD  
Committee Member

Accepted:

Kimberly Jacob Arriola, PhD, MPH  
Dean of the James T. Laney School of Graduate Studies

Date:

Decoding the Hidden Mechanisms of Soil Carbon Cycle in Response to Climate Change

By

Yaxi Du

B.S., University of California, Davis, 2022

Advisor: Debjani Sihi, PhD

An abstract of

A thesis submitted to the faculty of the

James T. Laney School of Graduate Studies of Emory University

in partial fulfillment of the requirements for the degree of

Master of Science

in Environmental Science 2024

## **Abstract**

### Decoding the Hidden Mechanisms of Soil Carbon Cycle in Response to Climate Change

By Yaxi Du

Climate change is rapidly redefining the biogeochemical dynamics of our planet, particularly in relation to soil organic carbon (SOC) storage and loss. We aim to isolate confounding elements and elucidate the principal mechanisms underpinning SOC dynamics under diverse environmental scenarios: warming (ambient, +1.5°C, and +2.5°C), and nutrient (nitrogen and phosphorus) and carbon addition treatments. Samples were collected from a low-latitude soil warming experiment where warming commenced in 2010 (Whitehall Forest, Athens, Georgia). Under laboratory conditions, we incubated soil samples (22 days) at their respective field temperatures at the time of sample collection. Core aspects of the soil carbon cycle, including particulate (and mineral-associated) organic carbon, microbial biomass carbon, and microbial necromass carbon, as well as critical processes such as soil microbial respiration and enzyme kinetics were examined. Our systematic evaluations helped separate the direct and indirect effects of warming (e.g., the inherent and apparent temperature sensitivity of SOC formation and loss). Our findings indicate that warming has a minor influence on soil carbon storage in substrate-limited ecosystems. However, as carbon and nutrient inputs increase, soil carbon loss accelerates. This study sheds light on the delicate balance between underlying mechanisms that control SOC dynamics in the face of climate change, emphasizing the nuanced interdependence of temperature, substrate resource availability, and soil carbon dynamics.

Decoding the Hidden Mechanisms of Soil Carbon Cycle in Response to Climate Change

By

Yaxi Du

B.S., University of California, Davis, 2022

Advisor: Debjani Sihi, PhD

A thesis submitted to the faculty of the  
James T. Laney School of Graduate Studies of Emory University  
in partial fulfillment of the requirements for the degree of  
Master of Science  
in Environmental Science 2024

## Acknowledgments

Completing this thesis has been both a journey and a testament to the incredible support and encouragement I have received. I extend my deepest gratitude to all who have contributed to this endeavor.

At the heart of my academic and research endeavors lies the Department of Environmental Science. Their patience, guidance, and belief in the importance of research have created an environment where curiosity thrives, and challenges are met with resilience. The comprehensive support system they have provided, encompassing both financial assistance for my research and opportunities for professional development through conference travel, has been invaluable. To the entire department, thank you for fostering a nurturing and supportive academic home.

I extend a special note of thanks to my advisor, Dr. Debjani Sihi. Her expertise, dedication, and insightful guidance have been instrumental in my research journey. Dr. Sihi's mentorship, characterized by patience and encouragement, has inspired me to push the boundaries of my knowledge and capabilities. Her unwavering support has been a guiding light, shaping both my research and my personal growth.

I would like to extend my gratitude to Dr. Jacqueline Mohan and her research group for granting me access to their site and sharing invaluable background information and details on the warming experiment. This collaboration has been essential to my research, offering unique insights and opportunities for data collection that greatly enriched my work. Additionally, I must acknowledge Dr. Shaunna Donaher, another committee member, for her time and constructive feedback. Her contributions have been instrumental in refining my research and enhancing its quality.

To my colleagues and friends in the lab, your spirit of collaboration, shared passion, and collective wisdom have enriched my experience beyond measure. Our countless discussions, collaborative efforts, and shared moments of both challenge and triumph have been pivotal to my journey. Thank you for the laughs, the support, and the invaluable lessons learned along the way.

Lastly, I owe an immeasurable debt of gratitude to my family. Your unconditional love, encouragement, and belief in my potential have been the bedrock of my journey. Your endless support and sacrifice have not only fueled my ambitions but also grounded me in my values. This accomplishment is as much yours as it is mine.

This thesis is a testament to the power of community, mentorship, and support. To everyone who has been a part of this journey, your contribution has been indispensable. Thank you for believing in me and for being part of this remarkable voyage.

## Table of Contents

1. Introduction
2. Material and Methods
  - 2.1. *Study Site and Field Sampling*
  - 2.2. *Experimental Design*
  - 2.3. *CO<sub>2</sub> Mineralization*
  - 2.4. *Soil Organic Content*
  - 2.5. *Physical Fractionation of SOM*
  - 2.6. *Microbial Biomass Carbon*
  - 2.7. *Amino Sugar Extraction and Microbial Residual C (necromass)*
  - 2.8. *Enzyme Kinetics*
  - 2.9. *Statistics*
3. Results
  - 3.1. *Temporal variability in CO<sub>2</sub> mineralization across treatments*
  - 3.2. *Carbon content distribution among soil organic matter (SOM) fractions*
  - 3.3. *Microbial biomass C (MBC) and residual C (necromass) response to incubation*
  - 3.4. *Enzyme activities and kinetics*
  - 3.5. *Correlations among measured soil properties before and after incubation*
4. Discussion
  - 4.1. *Substrate (C and nutrient) amendment but not temperature rise affects CO<sub>2</sub> mineralization*
  - 4.2. *Temperature but not treatment change affects SOC fractions*
  - 4.3. *MBC responses to temperatures and treatments*
  - 4.4. *Microbial residual C responses to temperatures and treatments*
  - 4.5. *Enzyme kinetics and activity response to treatments and temperatures*
  - 4.6. *Correlation matrix interpretations*
5. Conclusions and Future Implications
6. References
7. Appendix

## List of Figures

- Fig. 1: The components and processes of the soil carbon cycle.
- Fig. 2: U.S. map showing the study site.
- Fig. 3: A map of the Whitehall Forest soil warming experiment study site in Athens, Georgia.
- Fig. 4: Temporal dynamics of CO<sub>2</sub> mineralization across different treatments and temperatures.
- Fig. 5: Estimated total CO<sub>2</sub> mineralization under different treatments and temperatures.
- Fig. 6: Comparison of carbon content in soil organic matter (SOM) fractions before and after incubation.
- Fig. 7: Variations in microbial biomass carbon, MBC (mg C kg<sup>-1</sup> soil) before and after incubation.
- Fig. 8: Comparison of fungal, bacterial, and microbial residual C before incubation.
- Fig. 9: Variations in microbial residual carbon (C) across different temperatures and treatments after incubation.
- Fig. 10: Enzyme kinetic parameters (V<sub>max</sub> and K<sub>m</sub>) for six enzymes before incubation.
- Fig. 11: Enzyme activity (μM hr<sup>-1</sup> g<sup>-1</sup> soil) for AG and PHD before incubation.
- Fig. 12: Enzyme kinetic (V<sub>max</sub> and K<sub>m</sub>) parameters for all six enzymes responding to treatments and temperatures after incubation.
- Fig. 13: Enzyme activity (μM hr<sup>-1</sup> g<sup>-1</sup> soil) for AG and PHD after incubation in response to treatments and temperatures after incubation.
- Fig. 14: Correlation matrix before and after incubation.

## List of Tables

Table 1 List of soil extracellular enzymes assayed in this study.

Tables in Appendix:

Table 1: p-values for **initial** analyses in terms of temperatures from ANOVA.

Table 2: p-values for **post-incubation** analyses in terms of **treatments** from ANOVA.

Table 3: p-values for **post-incubation** analyses in terms of **temperatures** from ANOVA.

Table 4: p-values for **post-incubation** analyses in terms of **treatments : temperatures** from ANOVA.

Table 5: Detailed information for the field plots in Whitehall Forest, Athens, GA.

Table 6: Detailed information about lab equipment used in this study.

## 1. Introduction

Soil stores a large amount of terrestrial carbon (C) and can contribute to climate change mitigation (Li et al., 2014; Crowther et al., 2016; Machmuller et al., 2018; Tang et al., 2019; Pierson et al., 2021). Because of the size of the soil C pool (>2 times the amount of C stored in vegetation and atmosphere globally), a slight change in the C storage in the soil can have a big impact on the global atmospheric CO<sub>2</sub> concentration (Dash et al., 2019; Liang et al., 2019; Wood et al., 2019). Studying soil organic carbon (SOC) – the primary component of SOM – is essential for understanding the global C flux and climate mitigation mechanisms (Machmuller et al., 2018; Liang et al., 2019; Rocci et al., 2021). The stabilization of SOC can serve as a nature-based solution to climate change as it can lock away CO<sub>2</sub> from the atmosphere and store it in the soil for long-term, often decadal to millennial time-scale (Crowther et al., 2016; Tang et al., 2019; Pierson et al., 2021). Additionally, SOC is crucial for providing ecosystem services and environmental health, relating to the nutrients and services provided to other organisms (Hagerty et al., 2018; Tang et al., 2019; Wood et al., 2019; Rocci et al., 2021). Thus, an improved understanding of SOC dynamics is essential to evaluate the potential of soils to mitigate climate change and benefit the ecosystem.

Studies have shown that SOC pools (different stocks of organic C within the soil, such as particulates of organic carbon, POC; Mineral-associated organic C, MAOC, dissolved organic C, DOC) and fluxes (the processes that move C into, within, and out of the soil, such as decomposition and microbial respiration) are temperature-sensitive since nearly all underlying processes starting from belowground inputs of plant litter to microbial decomposition of soil organic matter (SOM) or soil CO<sub>2</sub> flux depend on temperature (Davidson and Janssens, 2006;

Dash et al., 2019; Tang et al., 2019). If rising temperatures promote faster respiration than photosynthesis, atmospheric CO<sub>2</sub> will increase and soil (and ecosystem) C stocks will fall (Davidson and Janssens, 2006; Tang et al., 2019). Thus, positive C-climate feedback will be generated, and that can further accelerate climate warming. Besides, the temperature sensitivity of SOC loss relies on environmental constraints, such as the supply of C and nutrient substrates (Xu et al., 2016; Dash et al., 2019). Management practices and climate can affect soil aggregate formation and soil fauna activities, which physically protect SOC. The SOC stabilization process can be related to climate warming as temperature can affect the chemical interaction between SOC and mineral surfaces (Dash et al., 2019). If climate warming can increase SOC stabilization, the feedback on climate change will be negative. However, the warming-induced loss of SOC can worsen the ongoing warming by creating positive feedback on climate change by increasing SOC losses by soil microbial respiration or soil CO<sub>2</sub> flux (Machmuller et al., 2018; Liang et al., 2019; Rocci et al., 2021). Therefore, it is imperative to better understand the feedback loop between soil C and climate change to develop effective policies for mitigating climate change.

Plant photosynthesis, root exudation, and animal waste deposition all serve as an input of C in the soil (Machmuller et al., 2018; Liang et al., 2019; Wood et al., 2019; Rocci et al., 2021). The C retrieved from plant litter is then converted and stored as different C pools (e.g., SOC fractions like POC and MAOC and microbial biomass C or MBC, Figure 1) inside the soil, where it is subjected to a suite of biological, chemical, and physical processes. Some processes include decomposition, respiration, stabilization, turnover, etc (Machmuller et al., 2018; Liang et al., 2019; Rocci et al., 2021). SOC can be categorized into particulate organic carbon (POC) and

mineral-associated organic carbon (MAOC) (Figure 1). POC represents the fraction of C derived from plant detritus, which is more vulnerable to microbial decomposition than MAOC, a more stable form of SOC (Machmuller et al., 2018; Liang et al., 2019; Vaughn and Torn, 2019; Rocci et al., 2021). The degradation of POC and microbial metabolism of the labile form of SOC (dissolved organic C, DOC) can result in heterotrophic CO<sub>2</sub> emissions. At the same time, the formation of MAOC fractions from plant residues and microbial necromass can help stabilize SOC as MAOC (Buckeridge et al., 2020, 2022). Destabilization of MAOC can also produce DOC, which if taken up by soil microbes, will release additional CO<sub>2</sub> by heterotrophic respiration to the atmosphere (Jilling et al., 2018; Pierson et al., 2021; Georgiou et al., 2022; Zhang et al., 2022). Most processes mentioned above are temperature-dependent and rely on other environmental factors, including soil moisture content and associated substrate (carbon and nutrient) availability. Understanding how C is sequestered in soil and how temperature influences the magnitude of each pool and flux allows us to target the “hotspot” for soil carbon storage and develop better management strategies for climate mitigation.

The conceptual model of the soil C cycle includes the major pools like SOC, DOC, microbial biomass C (MBC), and fluxes like decomposition of SOC to DOC, uptake of DOC by microorganisms, microbial production of enzymes that catalyze decomposition process, and turnover of microbial biomass that produces necromass (Allison et al., 2010; Wang et al., 2013; Buckeridge et al., 2022; Figure 1). Allison et al. (2010) proposed that the climate warming response depends on microorganisms' carbon use efficiency (CUE), so they added an enzyme function to the conventional model to demonstrate the effects of microbial biomass and enzyme kinetics in converting SOC to DOC. Wang et al. (2013) took more specific components into

account, such as splitting SOC into POC and MAOC. Wang et al. (2013) brought up the Q pool in their model, which is the adsorbed phase of DOC and represents mineral-associated organic matter (MAOM). Buckeridge et al. (2022) defined the microbial necromass continuum into four stages: production of necromass as a function of microbial turnover, recycling of necromass to SOC pool, stabilization into MAOC pool, and destabilization to DOC pool (and ultimately to CO<sub>2</sub> flux).

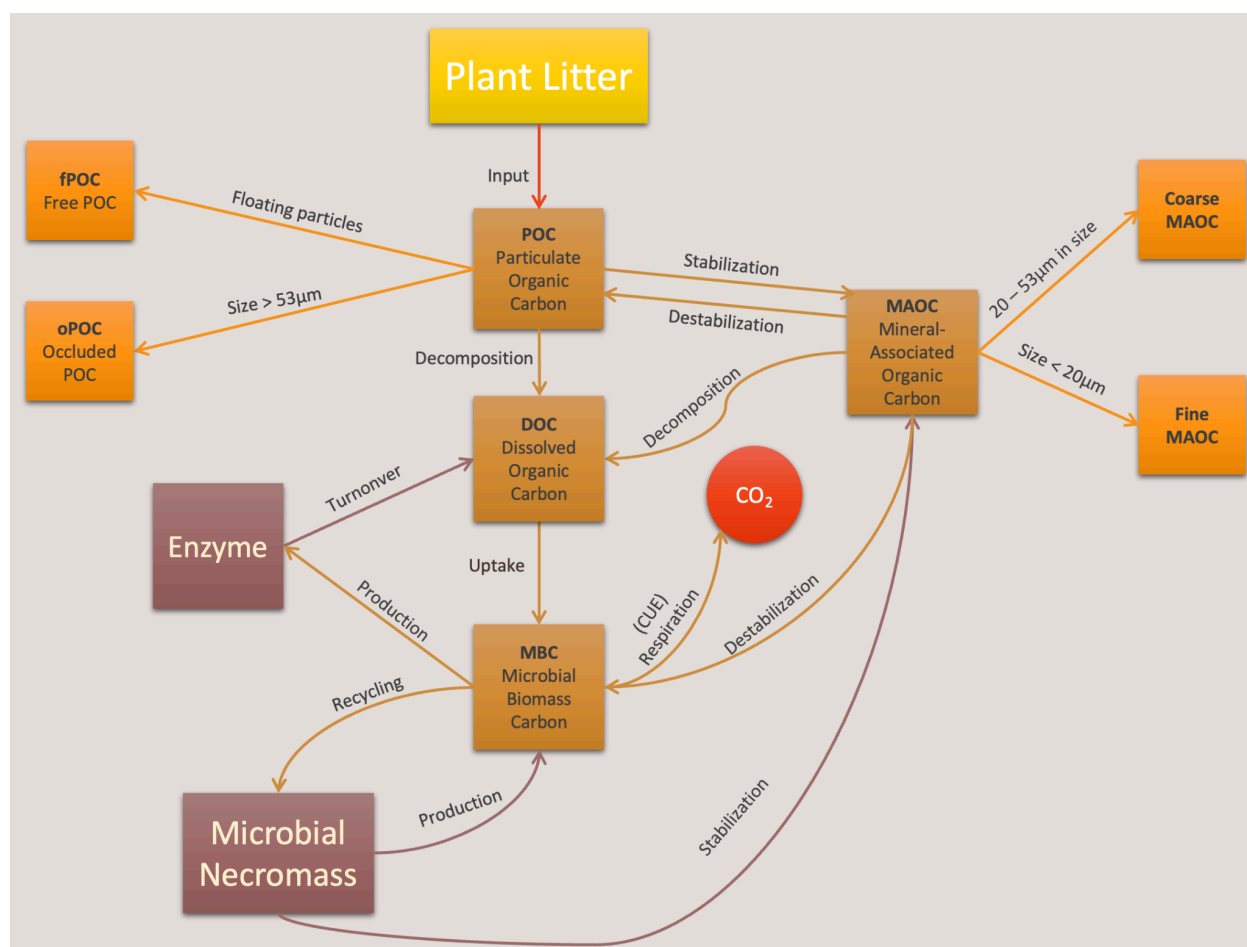


Fig. 1: The components and processes of the soil carbon cycle. Plant litter is represented in yellow box. Soil C pools are represented in light brown and orange boxes. Microbe-related products are represented in dark brown boxes. CO<sub>2</sub> is represented in red circle. Plant litter contributes to particulate organic carbon (POC), which could remain in the soil as free POC (fPOC) and could be protected within soil aggregates as occluded POC (oPOC). Interactions with soil minerals can result into stabilization of POC to mineral-associated organic carbon (MAOC), including

coarse MAOC and fine MAOC. fPOC are floating particles, and oPOC are particles with a size larger than 53  $\mu\text{m}$ . Coarse MAOC are particles with size between 53  $\mu\text{m}$  and 20  $\mu\text{m}$ , and fine MAOC are particles smaller than 20  $\mu\text{m}$ . C pools can be decomposed to dissolved organic carbon (DOC), which can be taken up by microbes (MBC). After their death, MBC can be converted to microbial necromass, which then can be stabilized to MAOC. CUE stands for carbon use efficiency, a critical ecological metric that quantifies the efficiency with which an organism, such as a microbe, converts assimilated C into biomass (measured as MBC). High CUE indicates that a greater proportion of C is being allocated to biomass growth rather than being respired as  $\text{CO}_2$  (Kuzyakov and Dijkstra, 2018; Li et al., 2018).

Inherent temperature sensitivity is anchored in the direct effects of warming on the kinetic prowess of soil enzymes, pivotal catalysts in the decomposition of soil organic matter (SOM). These enzymes accelerate or decelerate SOM breakdown, thus influencing soil C turnover as temperatures shift. Meanwhile, apparent temperature sensitivity unfolds through the observed warming responses amid environmental variables, such as soil moisture and substrate availability, intertwining in a complex dance that affects microbial access to C and nutrients, ultimately shaping soil C dynamics (Davidson and Janssens, 2006; Rocci et al., 2021). For instance, while increased temperatures are posited to diminish POC, the warming impact on stable SOC and MAOC remains minimal (Vaughn and Torn, 2019). Intriguingly, necromass production is more attuned to temperature shifts than its stabilization; this is chiefly because it is intrinsically linked to microbial growth, which is in turn governed by temperature-mediated microbial growth efficiency (Buckeridge et al., 2022). As temperatures rise, CUE is commonly expected to decline due to the heightened energetic demands placed on microorganisms for maintaining existing biomass (Cotrufo et al., 2013; Kuzyakov and Dijkstra, 2018). This constraint is rooted in the increased energy costs necessary to sustain existing microbial biomass under warming conditions (Cotrufo et al., 2013). Over time, this could lead to a gradual elevation

in the temperature sensitivity of CUE because of the selection pressures favoring microorganisms with higher maintenance costs (Li et al., 2014). Consequently, both the activation energy (or enzyme activity) and the turnover rate of SOC (or soil CO<sub>2</sub> flux) are projected to ascend with temperature up to a certain threshold (Machmuller et al., 2016, 2018).

Beyond warming effects, other environmental factors are also crucial. The soil nutrient level can influence the quantity and quality of plant input (Hagerty et al., 2018; Pierson et al., 2021), which in turn, could influence SOC pools and fluxes. Microbial CUE and MBC would decrease because the cost of nutrient acquisition would increase under low-nutrient conditions (Hagerty et al., 2018). However, these results are often subjected to high uncertainties due to other confounding factors (Falloon et al., 2011). For example, soil moisture content influences the availability of substrates (C and nutrients) for microbial growth and respiration, which in turn, impacts the soil C dynamic (Nocita et al., 2013; Moyano et al., 2018). Substrate availability can also influence the recycling of microbial necromass since the recycling efficiency is determined by the microbial growth rate (Liang et al., 2019).

Interactions between the direct and indirect effects of temperature change can impact soil C and climate feedback. Changes in enzyme capacity and enzyme-substrate interactions caused by warming might alter soil C responses to experimental warming because the temperature sensitivity of soil enzymes is one of the rate-limiting elements influencing SOM breakdown under warming (Burns et al., 2013; Schipper et al., 2014; Blagodatskaya et al., 2016; Ma et al., 2017; Fanin et al., 2022). Thermal adaptation of the decomposer community, encompassing changes in microbial physiology, community composition, structure, and activity of enzymes,

may also modify the warming response of soil microbial respiration (Bradford, 2013; Crowther and Bradford, 2013; Wei et al., 2014; Alster et al., 2016). Yet, there are differences in the assumptions behind soil microbial heat adaptability. Multi-phase patterns in soil respiration can also long-termly respond to warming, in which several variables interact to determine the timing and quantity of soil C loss (Melillo et al., 2017). Thus, the combined effects and the interactions between the inherent and apparent factors are hard to predict without direct empirical evidence.

Previous studies on warming responses to SOC generally focused on nutrient-rich soils in temperate or arctic/boreal climates, which makes it difficult to expand the findings of these studies to predict the warming response of nutrient-poor tropical/subtropical soils, which contain a major fraction of global soil C (Davidson, 2020; Nottingham et al., 2022). Besides, field research on the consequences of warming in tropical/sub-tropical ecosystems are infrequent due to the long-standing belief that tropical/sub-tropical soils are insensitive to warming as they are already subjected to high temperatures year-round, and are not vulnerable to additional warming. However, recent field warming studies showed mixed results (Machmuller et al., 2018; Nottingham et al., 2020). To address this knowledge gap, this project aims to explain the warming response of soil C cycle processes from a low-nutrient sub-tropical soil condition. The overall objective of this project is to demonstrate the effects of temperature and substrate (C and nutrient) levels on each soil C pool and flux. I hypothesize that warming will increase microbial biomass carbon (MBC) due to enhanced microbial activity and growth, which in turn will increase SOM decomposition rates. I also hypothesize that the warming response of SOM decomposition will be modulated by substrate (C and nutrient) availability, with higher nutrient levels amplifying the warming effect

on MBC. Concurrently, warming is predicted to increase CO<sub>2</sub> fluxes, reflecting heightened soil C loss. However, the availability of C and nutrient substrates may confound this response, potentially leading to a non-linear relationship between warming and CO<sub>2</sub> emissions. I hypothesize that the apparent temperature sensitivity of both soil C pools (e.g., MBC, POC, MAOC, necromass) and fluxes (e.g., enzyme-catalyzed decomposition of SOM and subsequent CO<sub>2</sub> emissions) will be higher than their inherent temperature sensitivity, due to the interactive effects of warming with varying environmental conditions such as substrate availability and nutrient levels.

## 2. Material and methods

### 2.1. Study site and field sampling

Samples were collected from the Whitehall Forest soil warming experiment study site in Athens, Georgia (Fig. 2). 2023 mean annual temperature of the site is 17.6 °C, and the mean annual precipitation is 126 cm (NOAA 2024). The soil is categorized as a subtropical (Ito and Wagai, 2017; Machmuller et al., 2018). The vegetation in the forest is mainly deciduous trees, such as *Quercus rubra*, *Q. alba*, *Liquidambar styraciflua*, and *Liriodendron tulipifera*, which emerged in the early 20th century after the cessation of farming activities on the land (Machmuller et al., 2018). The soils are classified as Typic Kanhapludults. The soil characteristics include low surface organic content, low fertility, and medium to low permeability. Soil pH is about 4.5, and the bulk density is 0.87g cm<sup>-3</sup> (Machmuller et al., 2016). To add warming treatments, heating cables were manually inserted at a 10 cm depth below the soil surface since 2010, which resulted in heating the biologically active layer (0-20 cm) (Machmuller et al., 2016). Triplicate plots have been maintained at different temperature levels – ambient, +1.5° C, and +2.5° C. Those warming

and ambient plots are surrounded by greenhouse plastics and soil warming cables are buried underneath. Additional plots (three replicates) have also been maintained for non-chambered control (NCC), indicating no greenhouse plastic around the plot or buried soil warming cables. All warming treatments (and NCC) were replicated in two habitats – forest and an adjacent manually-cleared canopy gap, to separate artifacts from above-ground (such as vegetation and the litter layer composed of fallen leaves) vs. below-ground components (such as the roots of plants and trees) of the ecosystem (Machmuller et al., 2018). Thus, there are a total of 24 field plots (Fig. 3).

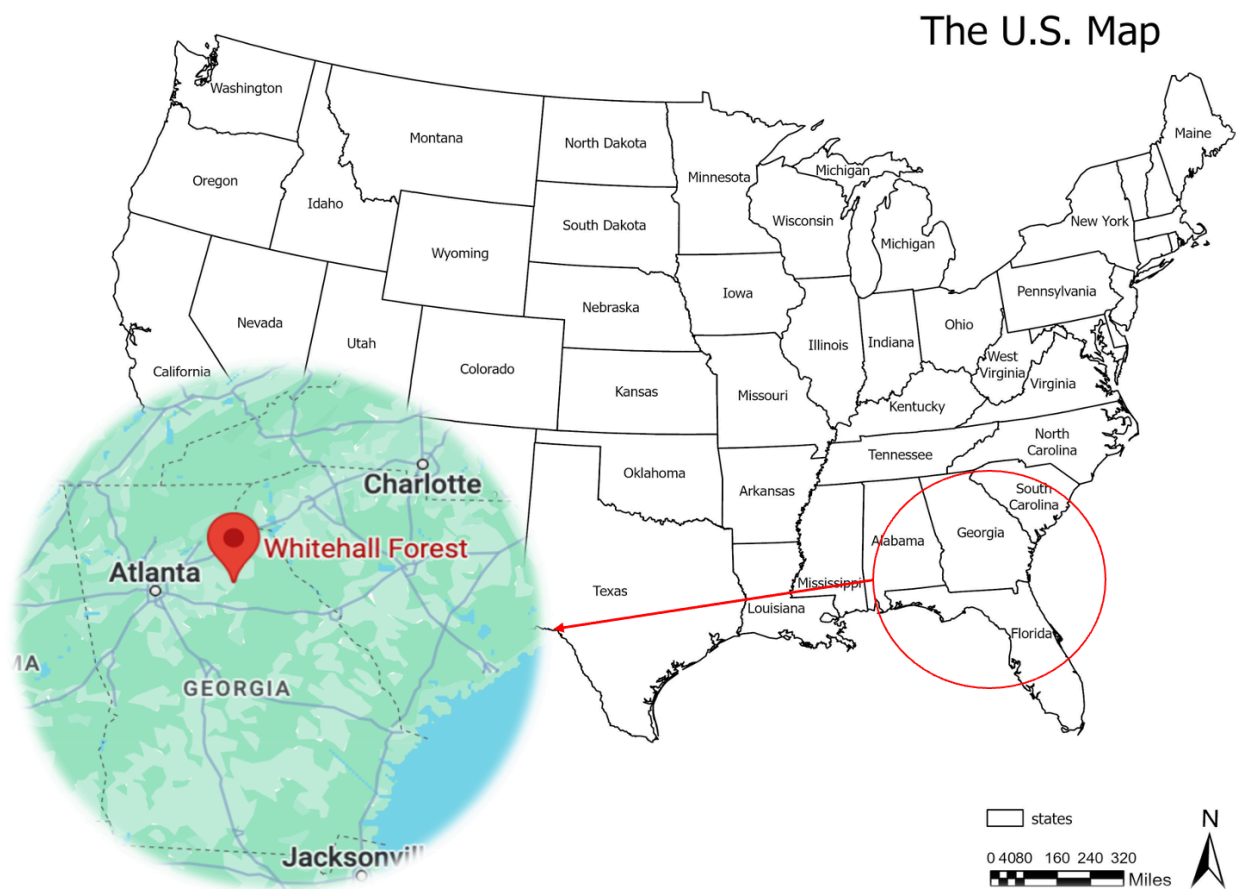


Fig. 2: U.S. map showing the study site. The soil samples were collected from a long-term warming experiment site at Whitehall Forest, Athens, GA.

The soil samples for wet-lab analyses were collected from all 24 plots (three field replicates for each plot) using a stainless soil sampler probe (inner diameter: 1 inch). The samples were collected from 20 cm soil depth – the most active layer for soil microbial activities (Gross and Harrison, 2019; Pellegrini et al., 2023). Each field replicate represents a composite of 3-5 samples. After sampling, the soils were kept in cooler boxes and transported back to the Sihi Biogeochemistry Lab at Emory University and stored at 4° C for further analysis and initiate the laboratory incubation study. In the lab, visible root fragments were removed by hand with latex gloves. To keep the soil condition at its original state, the soils were not sieved through a 2mm sieve upon retrieval. However, soils were sieved before performing each analysis separately. After retrieving the soil samples back in the lab, initial analyses on soil C pools, enzyme kinetics, and activities, and microbial necromass were performed by directly using the samples collected from the field. Three lab replicates on initial analyses using samples from all 24 plots were tested. Following the acquisition of the preliminary results, a 22-day incubation (from Oct. 30<sup>th</sup>, 2023 to Nov. 20<sup>th</sup>, 2023) was performed to separate direct and indirect effects of warming from confounding factors (C and nutrient substrates).

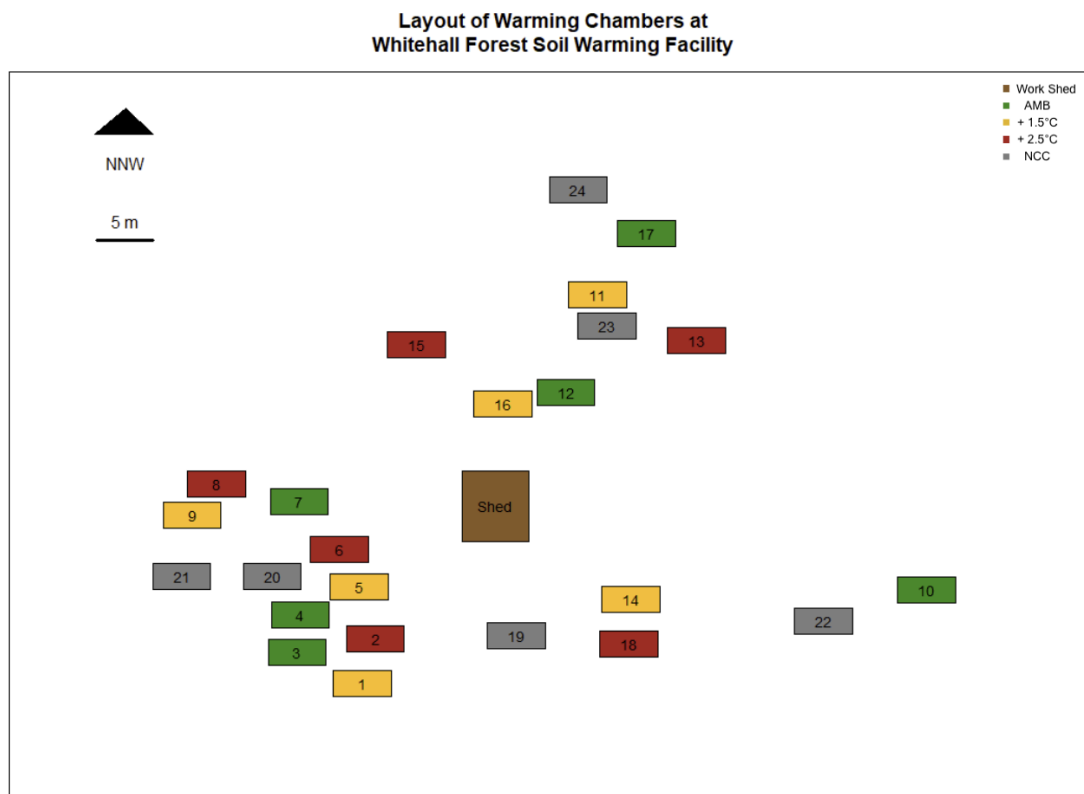


Fig. 3: A map of the Whitehall Forest soil warming experiment study site in Athens, Georgia. The numbers indicate actual plot numbers, and the colors represent the temperatures (brown is the work shed; green is the ambient plots; yellow is the 1.5°C above ambient plots; red is the 2.5°C above ambient plots; grey is the non-chambered plots). More detail information can be found in Appendix Tabel 5. Map source: Dr. Jacqueline Mohan's Lab at the University of Georgia.

## 2.2. Experimental Design

After performing initial analyses for all 24 plots, about 60 g of soil from ambient and each warming plot (all field plots except for NCC) were weighted into mason jars and incubated at three temperatures (25°C, 26.5°C, and 27.5°C) and three treatments representing three substrate types (C, N+P, N+P+C) for 22 days. After a 22-days of incubation, the same analyses as the initial analyses were performed on the soil C pool, enzyme kinetics and activities, and microbial

necromass. Each jar, containing the soil from one field plot, has only one lab replicate due to the limited sample amount, but three field plot replicates were measured. Soil moisture content was determined by the thermal gravimetric method (Reynolds, 1970). The moisture level was measured every two days while incubating to keep track of the soil water loss so that the substrate concentration would not be diluted or concentrated over time.

To separate the direct and indirect effects of warming, C and nutrient (N, P) substrates were added while performing the 22-day incubation. The substrates were added once at the beginning of the incubation period. N was added in the form of ammonium nitrate ( $\text{NH}_4\text{NO}_3$ ); P was added in the form of sodium dihydrogen phosphate ( $\text{NaH}_2\text{PO}_4$ ); C was added in the form of glucose ( $\text{C}_6\text{H}_{12}\text{O}_6$ ). The amount of each substrate added was calculated based on the field treatments in the study site and elsewhere. 0.164 mg N per g soil, 0.098 mg P per g soil, and 0.431 mg C per g soil were added to incubation jars.

### *2.3. CO<sub>2</sub> Mineralization*

For the incubation study, soil respiration was measured every two days until the readings reached a plateau. 1 to 2 ml of gas was collected using a plastic syringe directly from the incubated jars and injected into the Qubit CO<sub>2</sub> analyzer (Haney et al., 2018). The readings were given in ppm from the Qubit system and converted to  $\mu\text{g CO}_2$  per g dry soil by using the Ideal Gas Law and Henry's Law (Staudinger and Roberts, 1996; Woody, 2013). The detailed information of the lab machines and equipment can be found in Appendix Table 6.

### *2.4. Soil Organic C Content (SOC)*

Sieved (2mm) and oven-dried (105°C for 24 hours) soil samples were ground by using an 8000M Mixer Mill and stored at room temperature until analysis. The soil organic C content was measured through combustion using the ThermoFisher Scientific Elemental Analyzer.

### *2.5. Physical Fractionation of SOM*

Sieved (2mm) soils were physically fractionated to separate free-particulate organic matter (fPOM), occluded-particulate organic matter (oPOM), coarse MAOM, and fine MAOM according to Jilling et al. (2020) with minor modifications. Briefly, 10 g of sieved (2mm) and air-dried soil were dispersed in 50 ml water. Floating particles (fPOM) were retrieved by suction and cleaned on a 53 $\mu$ m sieve. The remaining soil and water were centrifuged at 10,000  $\times$  g (4200rpm) for 35 minutes. The supernatant was discarded. The soil and water suspension received an initial low-energy sonication (60J ml<sup>-1</sup>). The oPOM was passed through a 53 $\mu$ m sieve after sonication. The suspension recovered on the 53 $\mu$ m sieve was centrifuged at 10,000  $\times$  g (4200rpm) for another 35 minutes. The supernatant was discarded. The soil and water suspension received a second high-energy sonication (210J ml<sup>-1</sup>). The suspension was passed through a 20 $\mu$ m sieve. Materials recovered on the 20 $\mu$ m sieve were categorized as coarse MAOM and particles that were smaller than 20 $\mu$ m were categorized as fine MAOM. All the fractions were then dried at 105°C and stored for further analysis (Jilling et al., 2020). C contents for each soil fraction were calculated based on the total SOC and the fraction mass distribution.

### *2.6. Microbial Biomass C (MBC)*

Microbial biomass C was determined by chloroform fumigation followed by 0.5M K<sub>2</sub>SO<sub>4</sub> extraction. For fumigated extractions, 7 g of sieved (2mm) soils were mixed with 35 ml 0.5M

$K_2SO_4$  and kept in a desiccator for 24 hours with 20 ml boiled chloroform. Non-fumigated extractions were directly performed after 7 g of sieved (2mm) soils were mixed with 35 ml 0.5M  $K_2SO_4$ . Fumigated and non-fumigated extractions were filtered using Whatman No. 1 and total organic C (TOC) was determined using a Shimadzu TOC-L analyzer (Beck et al., 1997; Spohn et al., 2016). Microbial biomass was calculated as the difference in the concentration between the fumigated and non-fumigated extractions. An extraction efficiency factor of 0.45 has been calculated (Beck et al., 1997).

### *2.7. Amino Sugar Extraction and Microbial Residual C (necromass)*

Amino sugar was extracted based on the method described by Indorf et al. (2011). 400 mg sieved (2mm) and air-dried soil samples were mixed with 10 ml of 6M HCl and heated at 105°C for 6 hours. The samples were then filtered by using glass filters and Whatman No.1. A 1.5-ml aliquot of the mixture was evaporated to dryness at 60°C to remove HCl, redissolved in 1ml water, evaporated a second time, and redissolved in 1ml water. The solutions were then transferred to 1.5ml Eppendorf safe-lock tubes by using a 5ml syringe with 0.22 $\mu$ m filter units and were frozen at -20°C until delivered to Emory Woodruff Memorial Research Center for high-performance liquid chromatography (HPLC) analysis. Four amino sugars were targeted: muramic acid (MurN), glucosamine (GlcN), galactosamine (GalN), and mannosamine (ManN). Microbial residual C (i.e., microbial necromass within the soil matrix) was then quantified by converting the concentrations of each amino sugar from  $\mu$ M to  $mg\ g^{-1}$ . Fungal C ( $mg\ g^{-1}$ ) was calculated by  $(GlcN\ (mg) - 2 * MurN\ (mg) * 9) * 10^{-3}$ . Bacterial C ( $mg\ g^{-1}$ ) was calculated by  $MurN\ (mg) * 45 * 10^{-3}$ . Microbial residual C ( $mg\ g^{-1}$ ) was calculated by fungal C + bacterial C (Indorf et al., 2011; Joergensen, 2018).

### 2.8. Enzyme Kinetics

Eight hydraulic enzymes were assayed followed by the method described in Bell (2013) and Sihi et al. (2019). Six enzymes (BG, CB, AG, XYL, LAP, PHOS) were assayed at a range of substrate concentrations (100  $\mu\text{M}$  to 2000  $\mu\text{M}$ ) to measure enzyme kinetics (Table 1). Additionally, two other enzymes (NAG and PHD) were assayed at a 1000  $\mu\text{M}$  concentration level to determine maximum enzyme activity (Table 1). 2.75 g of sieved (2mm) soil was mixed thoroughly with 91 ml of 50 mM sodium-acetate buffer. The mixture was continuously stirred while 800  $\mu\text{l}$  of the soil slurry was pipetted into 96 deep well plates for incubation (1.5 hours at 35°C) and mixed with 200  $\mu\text{l}$  of substrate solutions. The standard curves for each sample were determined using 7-amino-4-methylcoumann (MUC) or 4-methylumbelliferone (MUB). The concentration range for the standards was 0  $\mu\text{M}$  to 100  $\mu\text{M}$ . After incubation, 250  $\mu\text{l}$  of the aliquot was transferred to black flat-bottomed 96-well plates. The fluorescence was determined using a fluorometric plate reader (Infinite M Nano+ Model: Infinite 200 pro) at 360 nm excitation and 460 nm emission (German et al., 2011; Bell et al., 2013; Sihi et al., 2019).

Enzyme activity was measured by  $\mu\text{mol}$  product released per hour per gram of soil. Enzyme kinetics was determined by  $V_{\text{max}}$  ( $\mu\text{M h}^{-1} \text{g}^{-1}$ ) and  $K_m$  ( $\mu\text{M L}^{-1}$ ) by using the Michaelis-Menten equation:  $V_0 = V_{\text{max}} * [S] / (K_m + [S])$ .  $V_0$  is the velocity of the reaction, expressed as a function of enzyme concentrations.  $V_{\text{max}}$  is the maximum reaction velocity.  $[S]$  is the substrate concentration, and  $K_m$  is the substrate concentration at  $0.5 * V_{\text{max}}$  (Sihi et al., 2019).

Table 1 List of soil extracellular enzymes assayed in this study.

Enzyme/Substrates	Abbreviation	Concentration(s)	Target substance	Standard Used for Calculation
<i>4-Methylumbelliferyl β-D-glucopyranoside</i>	BG	100 μM to 2000 μM	Labile C	MUB
<i>4-Methylumbelliferyl β-D-cellobioside</i>	CB	100 μM to 2000 μM	Labile C	MUB
<i>4-Methylumbelliferyl N-acetyl-β-D-glucosaminide</i>	NAG	100 μM to 2000 μM	N (& some C)	MUB
<i>4-Methylumbelliferyl phosphate</i>	PHOS	100 μM to 2000 μM	P	MUB
<i>Phosphodiesterase</i>	PHD	1000 μM	P	MUB
<i>4-Methylumbelliferyl β-D-xylopyranoside</i>	XYL	100 μM to 2000 μM	Stable C	MUB
<i>4-Methylumbelliferyl α-D-glucopyranoside</i>	AG	1000 μM	Stable C	MUB
<i>L-Leucine-7-amido-4-methylcoumarin hydrochloride</i>	LAP	100 μM to 2000 μM	N	MUC

## 2.9. Statistics

All the statistical analysis were performed by using R, version 4.1.0 (R Core Team, 2021). R-packages were used for data analysis: tidy (Wickham et al., 2024), dplyr (Wickham et al., 2023), stringr (Wickham, 2023), and visualization: ggplot2 (Wickham, 2016). Significant differences between different treatments were evaluated by Student's t-tests and Two-Way Analysis of variance (ANOVA) followed by Tukey PostHoc test. A 5% significance level (alpha <0.05) was used for statistical analyses.

### 3. Results

In general, there was enhanced CO<sub>2</sub> mineralization under nutrient and C additions across all temperature conditions, indicating increased microbial activity with substrate addition.

Temperature elevation slightly increased cumulative soil respiration, with the highest increase observed under the highest temperature treatment. The resilience of certain soil C fractions was highlighted, like oPOC, to environmental changes. Microbial biomass and necromass varied with temperature and treatments (i.e., substrate types), showing complex microbial dynamics. Enzyme activities revealed nuanced interactions between microbial processes and environmental factors, underscoring the complexity of soil C responses to climate change drivers. All the ANOVA (Analysis of variance) results can be found in the Appendix (Table 1-4).

#### *3.1. Temporal variability in CO<sub>2</sub> mineralization across treatments*

During the 22-day incubation, headspace CO<sub>2</sub> concentrations followed a typical microbial growth curve indicating microbial activities at the lag phase (~2-3 days), exponential or log phase (~5-6 days), and stationary phase (~ 13-15 days). We stopped the experiment when headspace CO<sub>2</sub> concentrations reached a plateau indicating soil respiration rates reached a steady state (Fig. 4). In all three temperature conditions (AMB at 25°C, +1.5°C at 26.5°C, +2.5°C at 27.5°C), the temporal pattern was similar but pronounced peaks were observed in the N+P+C treatment, suggesting an enhanced microbial activity due to nutrient and C addition (Fig. 4). This peak was notably higher than N+P treatment. With C addition alone, soil respiration increased but less than N+P+C treatment. Figure 5 summarizes the total CO<sub>2</sub> mineralization across the study period. Temperature elevation has a slight impact on cumulative soil respiration, with the highest temperature treatment (27.5°C) consistently resulting in greater CO<sub>2</sub> efflux across all

nutrient amendments. Notably, the N+P+C treatment exhibited the highest CO<sub>2</sub> mineralization rates at all temperature treatments, and the N+P treatment had the lowest. The N+P treatment did not vary much compared to the treatment with no amendment (expressed as None).

The ANOVA test was conducted to examine the effect of treatments and temperatures on CO<sub>2</sub> mineralization (Appendix Tables 2-4). The ANOVA showed a highly significant effect of the treatment ( $p < 2e-16$ ), with an F value of 44.705. However, the temperature factor alone did not show a significant effect ( $p = 0.49$ ), and the interaction between treatment and temperature was also not significant ( $p = 0.69$ ). Tukey's HSD test was then used to conduct pairwise comparisons between the treatment means to identify which specific treatments differ from each other. The results indicate significant differences between several treatment pairs. The N+P treatment significantly reduced CO<sub>2</sub> mineralization compared to the C treatment with a mean difference of -15.08 mg C g<sup>-1</sup> soil ( $p < 0.000001$ ). The difference between C and N+P+C treatment was not statistically significant ( $p = 0.16$ ). The comparison between N+P and N+P+C treatments and between None and N+P treatments also showed significant differences ( $p < 0.000001$ ).

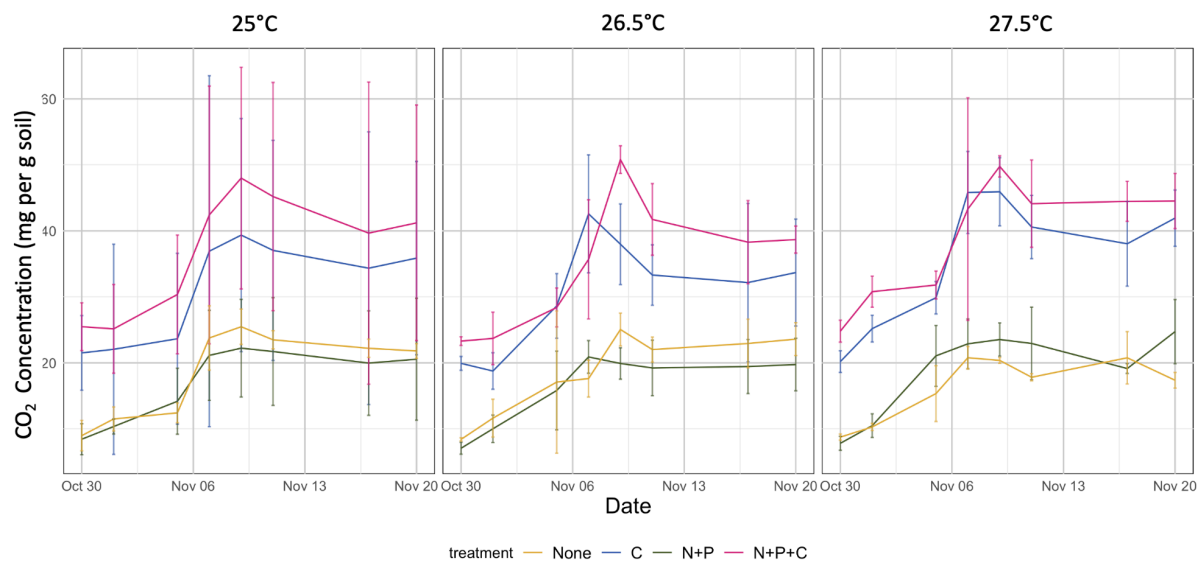


Fig. 4: Temporal dynamics of CO<sub>2</sub> mineralization across different treatments and temperatures. CO<sub>2</sub> efflux was measured and calculated in mg CO<sub>2</sub> per g soil from October 30<sup>th</sup>, 2023 to November 20<sup>th</sup>, 2023. Temperatures include ambient at 25°C (AMB), 26.5°C (+1.5°C), 27.5°C (+2.5°C), treatments include no amendments (None), carbon addition (C), nutrient (nitrogen and phosphorus) addition (N+P), and both carbon and nutrient addition (N+P+C). Error bars represent standard errors, highlighting the temporal trend of CO<sub>2</sub> under different treatments. A significant effect of the treatment was observed ( $p < 2e-16$ ).

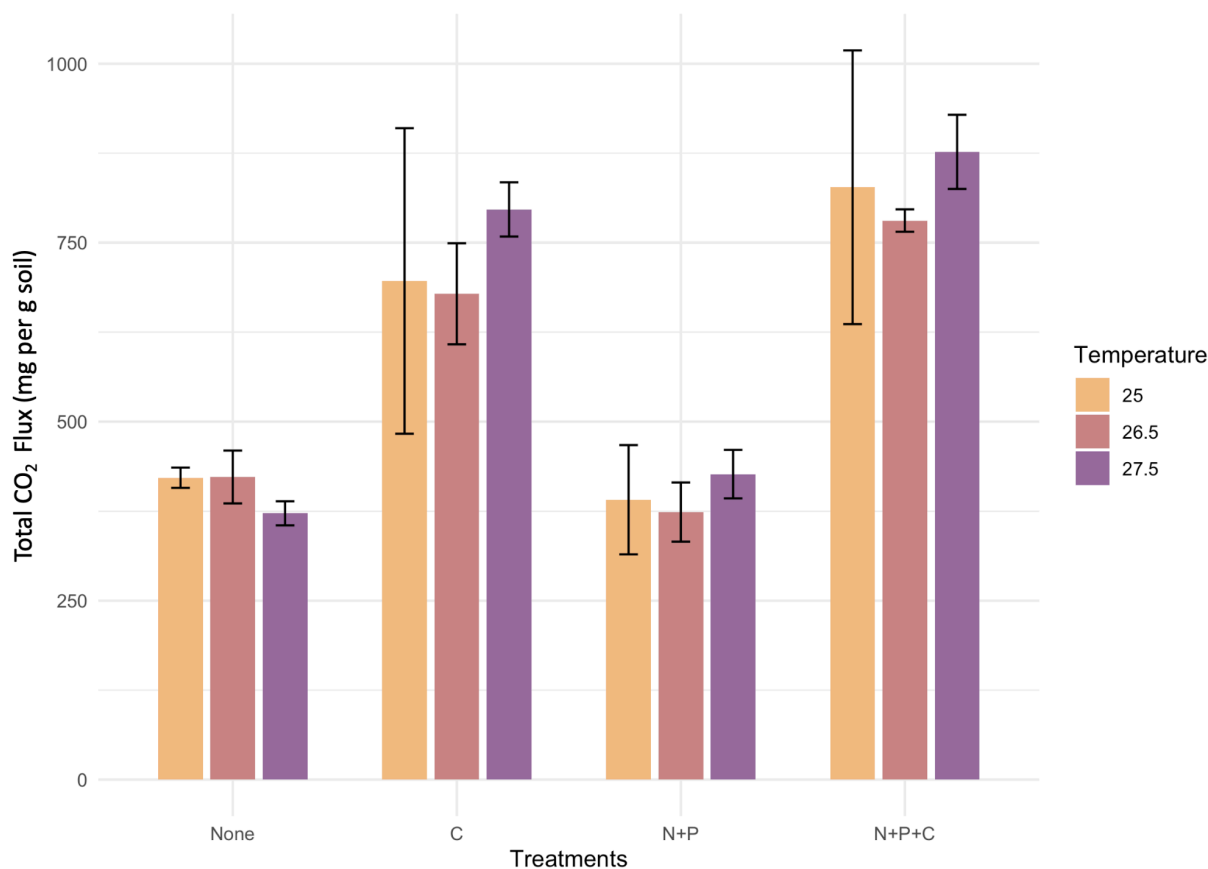


Fig. 5: Estimated total CO<sub>2</sub> mineralization under different treatments and temperatures. CO<sub>2</sub> efflux was measured and calculated in mg CO<sub>2</sub> per g soil. A linear interpolation technique was adopted to estimate the cumulative value of headspace CO<sub>2</sub> concentrations over the entire incubation period. The colors of the bars represent the temperatures. The error bars denote the standard errors, which illustrate the variability within each treatment category.

### 3.2. Carbon content distribution among soil organic matter (SOM) fractions

The particulate organic carbon, both free (fPOC) and occluded (oPOC), demonstrated notable C presence. oPOC accounted for the majority of the measured C content across the temperatures and treatments before and after incubation, while fPOC was the lowest (Fig. 6). The coarse MAOC and fine MAOC contained considerably lower C quantities, underscoring the

contribution of organic matter fractions to stable soil C pools. Soil samples from 27.5°C plots contain the most oPOC among all other temperatures for pre- and post-incubation.

Although fPOC contents were negligible, the ambient (25°C) conditions contained a larger portion compared to 26.5°C and 27.5°C scenarios for post-incubation ( $p = 0.03$ , Fig. 6B). There was a decrease in oPOC at 25°C after incubation (from 25.85 g C kg<sup>-1</sup> soil to 13.12 g C kg<sup>-1</sup> soil). No large differences were observed among treatments after incubation (Appendix Table 2-4). However, there was a slight increase in oPOC contents for nutrient and C additions (C, N+P, N+P+C) compared to no amendment (Fig. 6C). Coarse MAOC and fine MAOC remained relatively consistent across different temperatures and treatments. In general, non-chambered control (NCC) had a much lower C content compared to AMB.

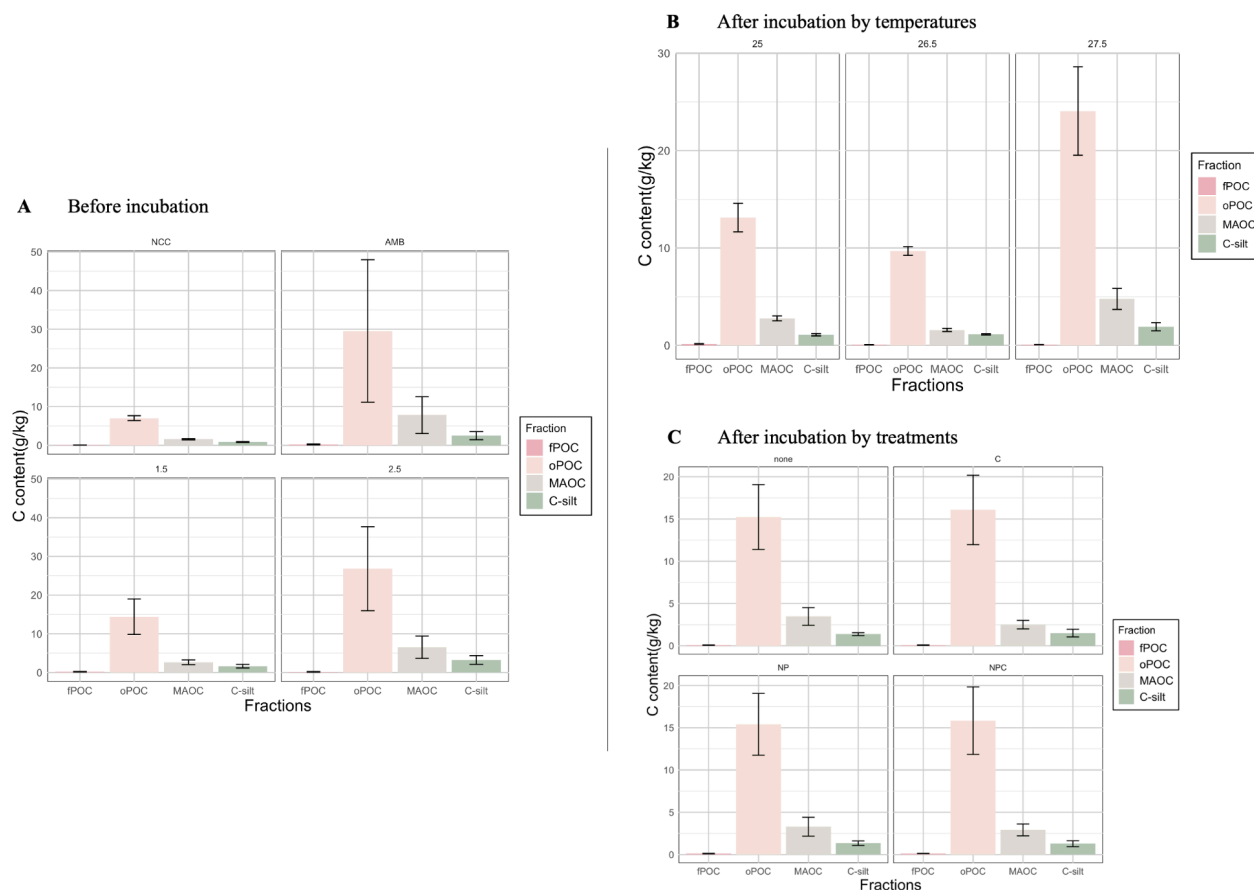


Fig. 6: Comparison of carbon content in soil organic matter (SOM) fractions before and after incubation. **A** Figure on the left panel displays the C content of different SOM fractions before incubation under different temperatures. *P*-values for ANOVA are larger than 0.1. **B** Figure on the top right panel illustrates the carbon content in the same SOM fractions after incubation at different temperature levels (25°C, 26.5°C, and 27.5°C). **C** The bottom right panel delineates the carbon content after incubation by treatment types (None, carbon addition (C), nitrogen and phosphorus addition (N+P), and combined nitrogen, phosphorus, and carbon addition (N+P+C)). C content is in g C kg<sup>-1</sup> soil. fPOC has a significant difference among temperatures ( $p < 0.05$ ).

### 3.3. Microbial biomass C (MBC) and residual C (necromass) response to incubation

Before incubation, the MBC levels spanned a broad range, with no clear pattern detected across the non-chambered control (NCC) and the different temperature treatments (Fig. 7A). The MBC data revealed intriguing trends after incubation. While ANOVA indicated no statistical

significance, suggesting that the observed changes in MBC are within the natural variability of the system, some patterns are noteworthy (Appendix Table 1). At warmer temperatures of 26.5°C and 27.5°C, MBC increased in plots with substrates addition (C, N+P, N+P+C) compared to those without any amendments (Fig. 7B). While observing across the treatments regardless of temperatures, plots with N+P and N+P+C treatments displayed a decrease in MBC, with N+P treatments tend to have the lowest MBC across the board. A comparison between pre- and post-incubation conditions indicates a general tendency for MBC to be higher after incubation.

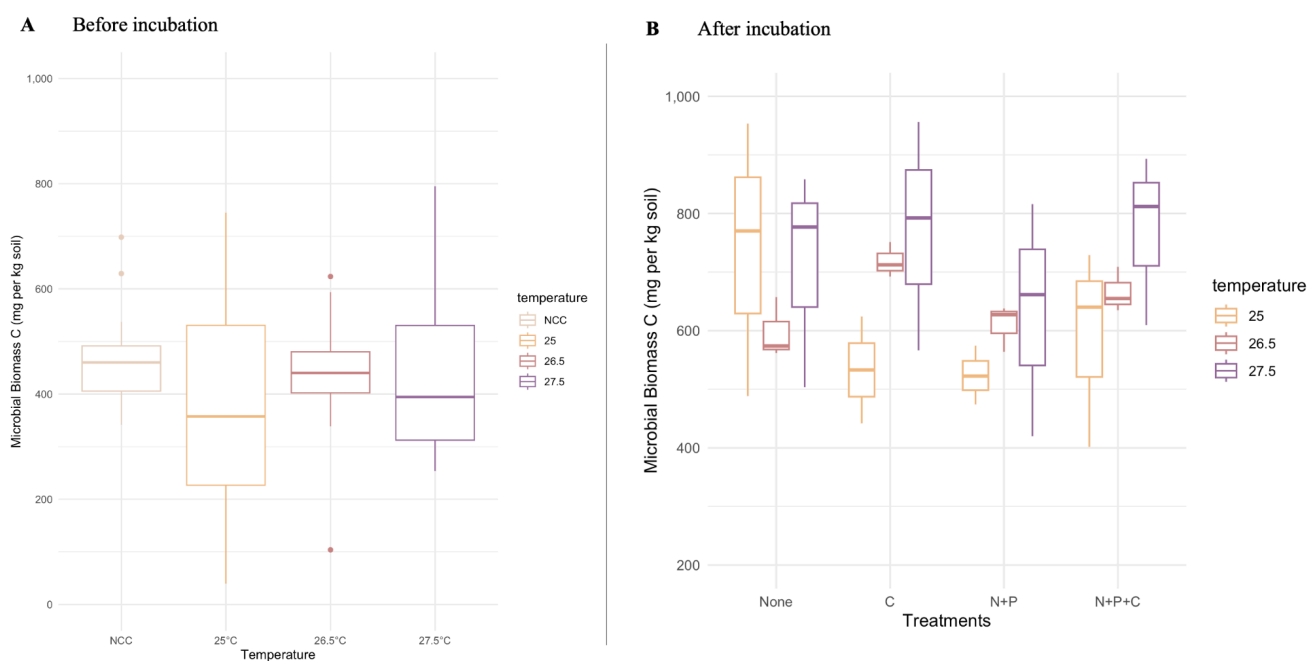


Fig. 7: Variations in microbial biomass carbon, MBC ( $\text{mg C kg}^{-1}$  soil) before and after incubation. **A** Figure at the left panel depicts the distribution of MBC before incubation. **B** Figure at the right panel illustrates the MBC values after incubation, grouped by substrate treatments. The data indicates an increase in MBC with carbon addition at higher temperatures (26.5 and 27.5°C) compared to other treatments, which tend to decrease MBC irrespective of the temperature when compared to the no amendment control. N+P treatment generally exhibits the lowest MBC across temperatures. Box plots show median values with interquartile ranges, and whiskers represent the data range

excluding outliers, which are plotted as individual points. *P-values* for ANOVA are larger than 0.1 (Appendix Tables 2-4).

Microbial residual C, which indicates the microbial necromass pool, tends to be the highest at 26.5°C before incubation (a mean of 0.433 mg C g<sup>-1</sup> soil, Fig. 8). Bacterial residual C demonstrated a robust presence across both environmental conditions, suggesting a greater contribution (or higher turnover rate) of bacterial biomass to total microbial residual C pool in comparison to fungi. Notably, the necromass was reduced when the temperature increased to 27.5°C (a mean of 0.426 mg C g<sup>-1</sup> soil, Fig. 8). However, the differences were not significant ( $p > 0.1$ ). Contrary to the results before incubation, 27.5°C temperature tended to have the highest microbial residual C compared to 25°C and 26.5 °C after incubation. When comparing across treatments, N+P+C had the highest microbial residual C despite the temperature differences (Fig. 9A). In contrast, bacterial C did not show a distinct pattern that correlated with the temperature gradients post-incubation (Fig. 9B). However, a general trend of increasing bacterial C concentration with rising temperatures was observed. Fungal C content remained a relatively constant pattern across the treatments and temperatures, both before and after incubation (Figs. 8&9C). For the ANOVA test, there were significant effects for temperature on both microbial residual C and fungal C ( $p = 0.044$  and  $0.038$ , respectively) (Appendix Table 3).

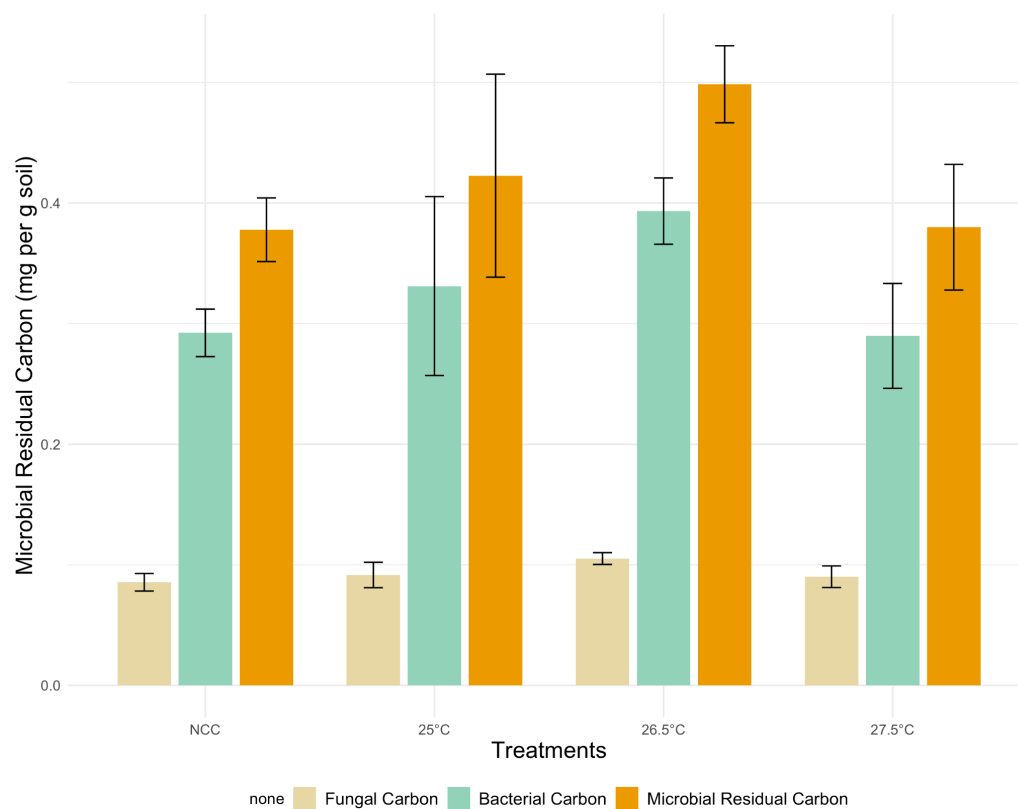


Fig. 8: Comparison of fungal, bacterial, and microbial residual C before incubation. The figure illustrates the concentrations of fungal C (light brown bars), bacterial C (green bars), and microbial residual C (dark brown bars) across different temperatures. The microbial residual C, indicative of the necromass content, displays a marked increase at the 26.5°C treatment. Microbial residual C is the sum of bacterial and fungal C. C concentration expressed as mg C g<sup>-1</sup> soil. *P-values* for ANOVA are larger than 0.1 (Appendix Table 1).

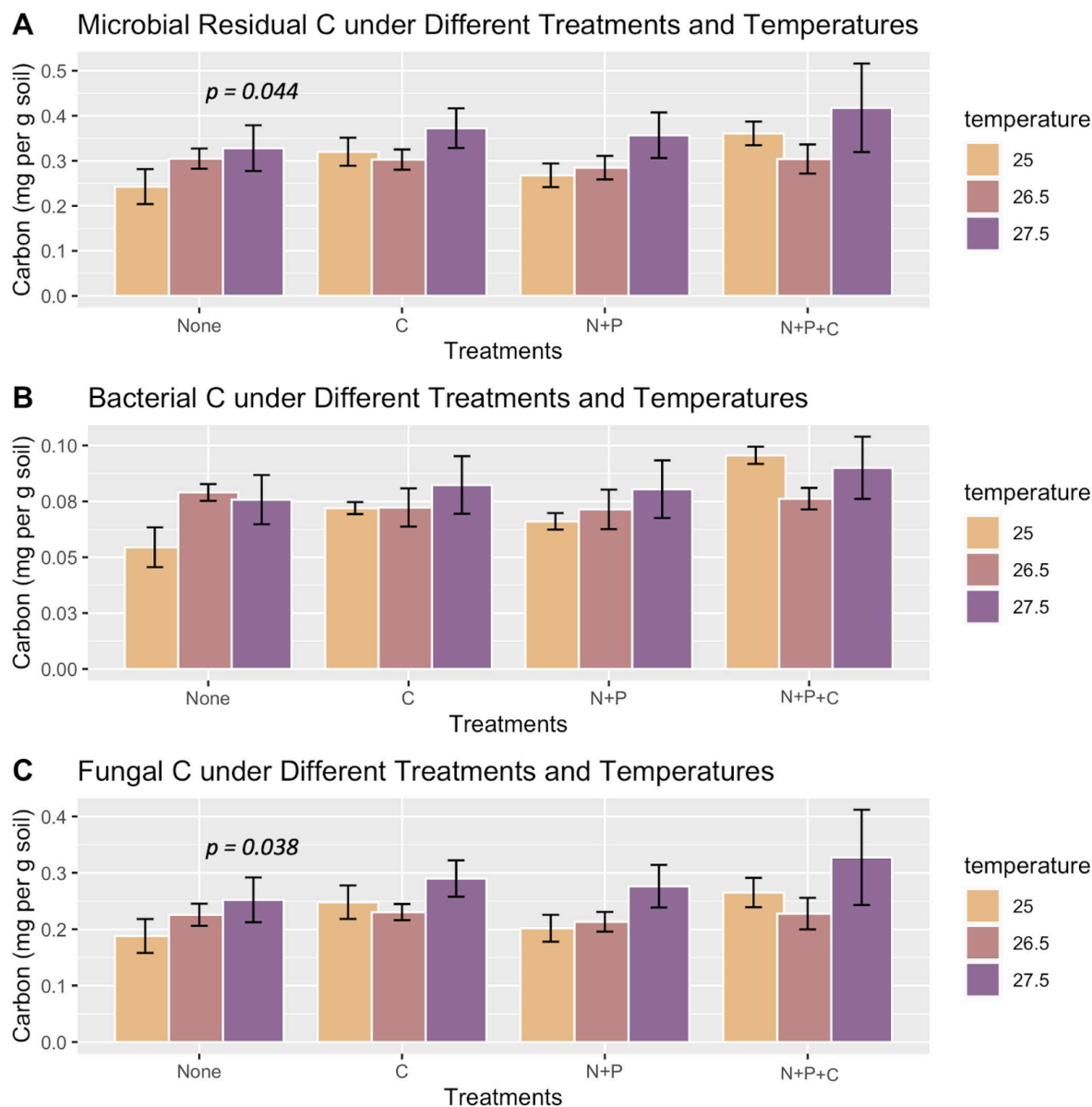


Fig. 9: Variations in microbial residual carbon (C) across different temperatures and treatments after incubation. **A** Microbial residual C under various treatments (none, C, N+P, and N+P+C) and temperature conditions (25°C, 26.5°C, and 27.5°C), showing the highest concentration at 27.5°C across treatments. **B** Bacterial C distribution under the same treatments and temperatures, indicating a less distinct pattern compared to microbial residual C, but with a general trend of increasing concentration with rising temperatures. **C** Fungal C content across treatments and temperatures, with a relatively uniform distribution, suggesting a more stable fungal C pool in response to the tested

conditions. There were significant effects for temperature on both microbial residual C and fungal C ( $p = 0.044$  and  $0.038$ , respectively) (Appendix Table 3).

### 3.4. Enzyme activities and kinetics

The enzymatic activities and kinetic parameters of soil enzymes were evaluated under different treatments, examining both the maximum reaction velocity ( $V_{max}$ ) and the Michaelis-Menten constant ( $K_m$ ) before soil incubation. BG and CB are crucial for the degradation of labile C compounds and exhibit a discernible response to temperature variations. The highest  $V_{max}$  for PHD both enzymes was observed at  $26.5^\circ\text{C}$  (Fig. 10A-B). A pronounced decrease in  $V_{max}$  at  $27.5^\circ\text{C}$  was indicative of diminishing enzyme efficiency at the upper end of the tested temperature range. LAP is associated with nitrogen cycling within the soil matrix, demonstrating a relatively stable  $V_{max}$  and  $K_m$  across the temperature treatments (Fig. 10D-J). PHOS showed a slight uptick in  $V_{max}$  within NCC (Fig. 10F). XYL displayed a significant increase in  $V_{max}$  in the NCC treatment (Fig. 10C).  $K_m$  value followed a similar trend as  $V_{max}$  for BG and CB (Fig. 10G-H), indicating a higher substrate affinity at the lower temperature of  $26.5^\circ\text{C}$  and decreasing affinity as temperatures rise. In contrast, the  $K_m$  values of LAP, NAG, and PHOS did not demonstrate a consistent pattern across treatments, suggesting varied affinity to their respective substrates that were not directly related to temperature levels (Fig. 10J-M). PHD tended to have much higher activities than AG in general (Fig. 11). While the highest activity of PHD was observed in NCC, AG activity showed a decreasing trend with increasing temperature. According to the ANOVA result, there were significant temperature effects on BG ( $V_{max}$ ) and LAP ( $V_{max}$ ) ( $p = 0.08$  and  $0.023$ , respectively) as well as AG and PHD enzyme activities ( $p = 0.018$  and  $0.006$ , respectively) (Appendix Table 3).

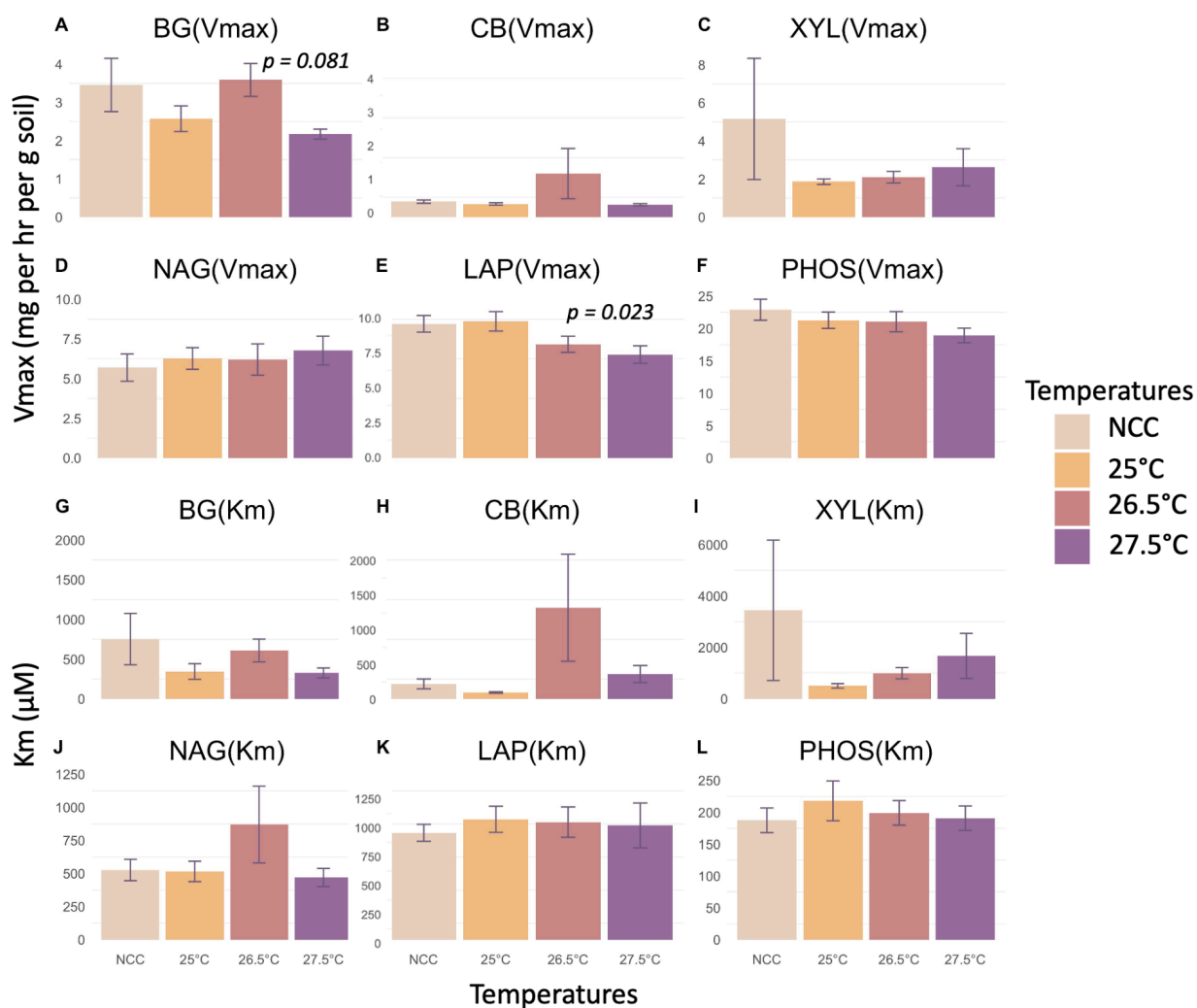


Fig. 10: Enzyme kinetic parameters (Vmax and Km) for six enzymes before incubation. Upper panels (A-F) represent maximum velocity (Vmax as  $\mu\text{M hr}^{-1} \text{g}^{-1} \text{soil}$ ) for the enzymes under different temperatures. Bottom panels (G-L) represent the Michaelis-Menten constant (Km as  $\mu\text{M}$ ) for enzymes, indicating substrate affinity across temperatures. Higher Km indicates a decreased enzyme-substrate affinity, while lower values suggest a more efficient substrate utilization. There were significant temperature effects on BG (Vmax) and LAP (Vmax) ( $p = 0.081$  and  $0.023$ , respectively).

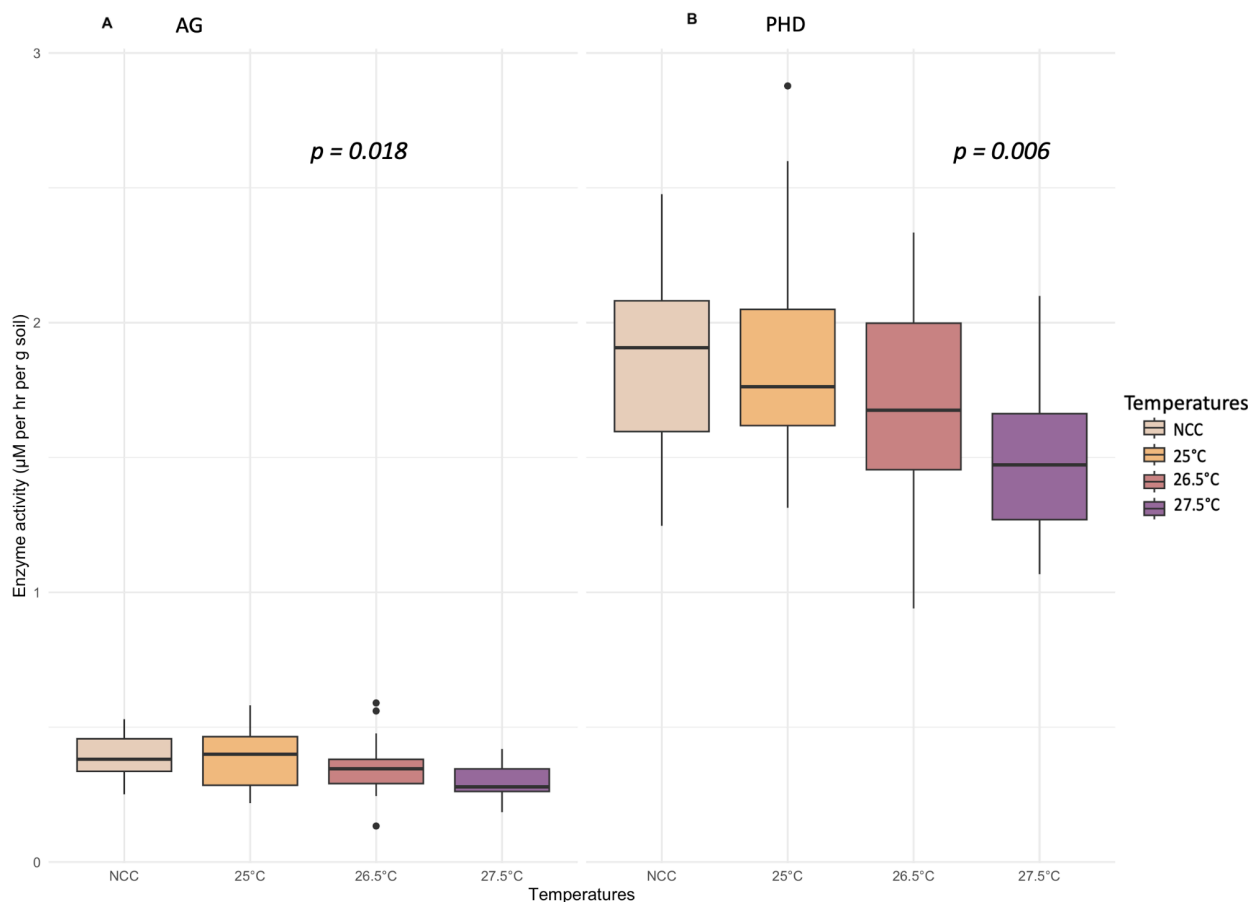


Fig. 11: Enzyme activity ( $\mu\text{M hr}^{-1} \text{g}^{-1} \text{soil}$ ) for AG and PHD before incubation. Left panel (A) represents the enzyme activity of AG across temperatures. The right panel (B) represents the enzyme activity of PHD across temperatures. There were significant temperature effects on AG and PHD enzyme activities ( $p = 0.018$  and  $0.006$ , respectively).

The post-incubation assays revealed nuanced enzyme-specific responses to temperature and substrate (C and nutrient) addition treatments. Note the absence of BG at 25°C due to inadequate data for fitting the Michaelis-Menten model for enzyme kinetics, underscoring the need for a broader substrate concentration range for future assays. For BG, the  $V_{\text{max}}$  reached the highest at N+P+C treatment and 27.5°C compared to 26.5°C. Simply C addition decreased the  $V_{\text{max}}$  of BG (Fig. 12A). In contrast, the  $V_{\text{max}}$  of CB reached the highest at 26.5°C under C addition (Fig. 12B). XYL, interestingly, reached the highest  $V_{\text{max}}$  at 25°C under N+P+C treatment (Fig. 12C).

On the other hand, the trend of LAP, NAG, and PHOS remained relatively consistent across temperatures and treatments:  $V_{max}$  reached the highest at 25°C for all three substrates (Fig. 12D-F). The  $V_{max}$  of PHOS showed a clear decreasing trend as the temperature increased. The  $K_m$  values did not align with the patterns observed for  $V_{max}$  in a temperature-dependent manner. BG exhibited a significant decrease in  $K_m$  with increasing temperatures, and N+P treatment at 27.5°C hit the lowest  $K_m$  for BG (Fig. 12G). However, the  $K_m$  of CB, XYL, LAP, NAG, and PHOS displayed a similar pattern as their  $V_{max}$  (Fig. 12). Enzyme activity for AG was the highest under N+P+C treatment at 27.5°C and that at 25°C was negligible (Fig. 13A-B). The activity of PHD at 25°C was surprisingly high compared to other temperatures and to that of AG (Fig. 13C). Under N+P+C treatment, PHD activity reached the highest at 27.5°C (Fig. 13D).

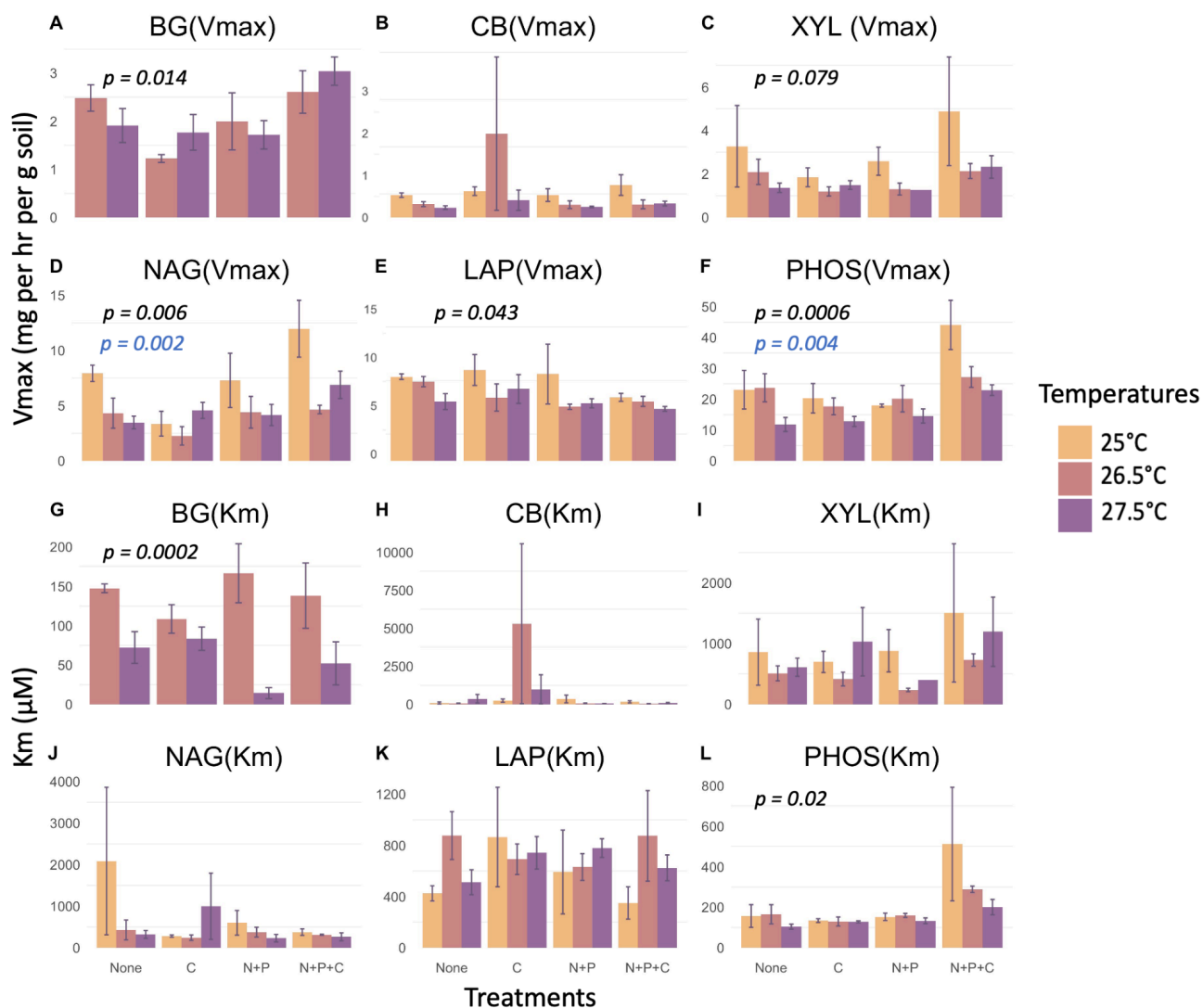


Fig. 12: Enzyme kinetic ( $V_{max}$  and  $K_m$ ) parameters for all six enzymes responding to treatments and temperatures after incubation. Upper panels (A-F) represent maximum velocity ( $V_{max}$  as  $\mu\text{M hr}^{-1} \text{g}^{-1} \text{soil}$ ) for the enzymes under different treatments and temperatures. Bottom panels (G-L) represent the Michaelis-Menten constant ( $K_m$  as  $\mu\text{M}$ ) for enzymes, indicating substrate affinity across treatments and temperatures. Note the absence of BG at 25°C due to inadequate data for fitting the Michaelis-Menten model for enzyme kinetics, underscoring the need for a broader substrate concentration range for future assays. p-values shown in black are treatment effects, and p-values shown in blue are temperature effects.

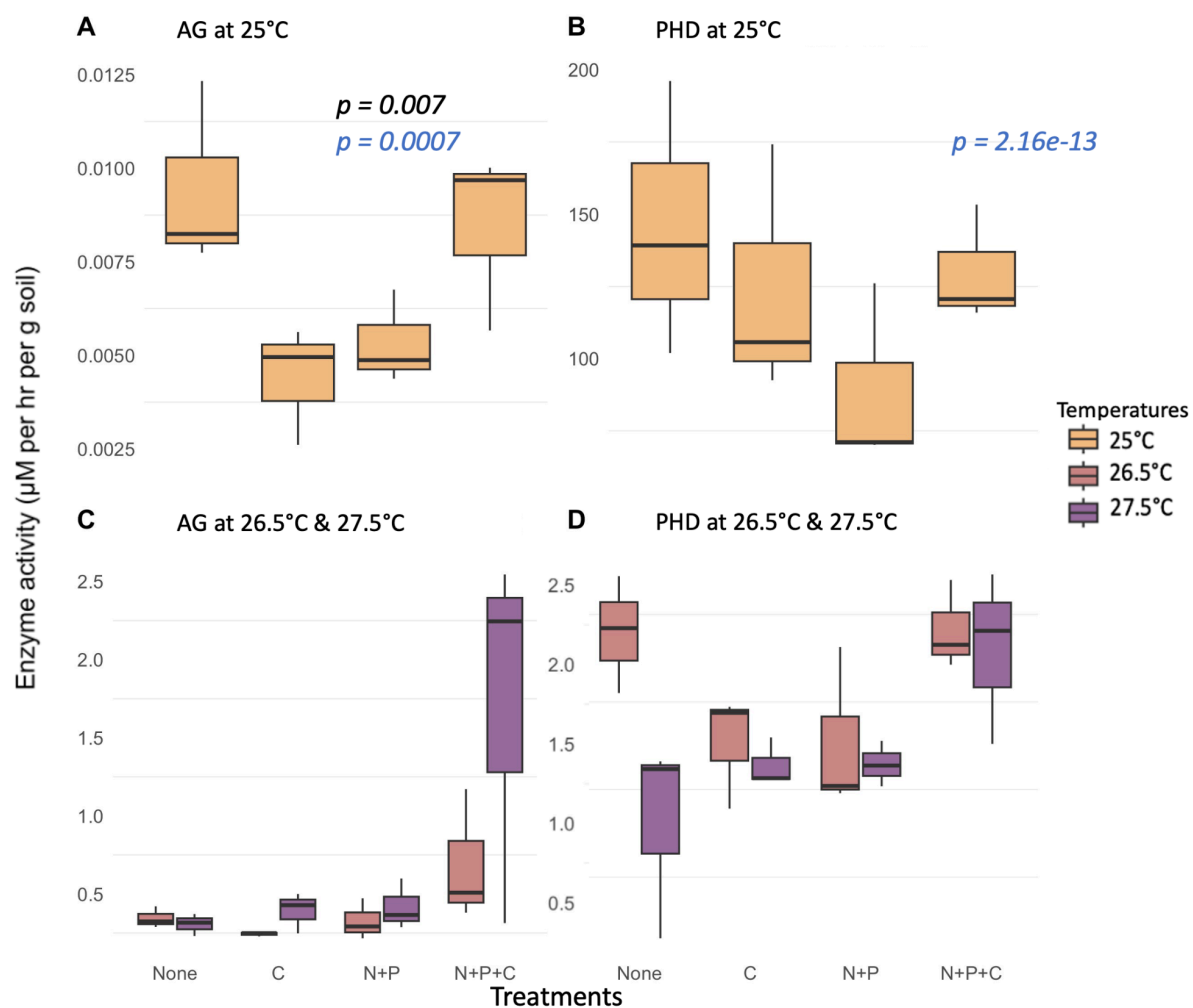


Fig. 13: Enzyme activity ( $\mu\text{M hr}^{-1} \text{g}^{-1} \text{soil}$ ) for AG and PHD after incubation in response to treatments and temperatures after incubation. Left panels (A, C) represent the activity of AG and right panels (B, D) indicate the activity of PHD. The top panels represent the activity of AG (A) and PHD (C) across treatments at 25°C. The bottom panels represent the activity of AG (B) and PHD (D) across treatments at 26.5°C and 27.5°C. p-values shown in black are treatment effects, and p-values shown in blue are temperature effects.

### 3.5. Correlations among measured soil properties before and after incubation

Correlations before incubation are generally weaker, suggesting that the relationships between soil properties and enzyme activities are less defined before incubation (Fig. 14A). The matrix

reveals that the associations between soil properties such as fungal C, bacterial C, microbial residues C, and different C fractions of SOM such as fPOC and MAOC are not as strong as they would be after the incubation process. Interactions between MBC and fungal C and microbial residue C are more pronounced compared to bacterial C. There are discernible yet moderate correlations between enzymes involved in the decomposition of organic matter, such as BG, CB, and NAG, and the soil C pools. The kinetic parameters of these enzymes, particularly the maximum velocity ( $V_{max}$ ), do not show strong connections to the SOM fractions or MBC.

After incubating soils, stronger correlations (dark blue) among enzyme activities (e.g., PHOS\_Vm, XYL\_Vm, NAG\_Vm, etc.) suggest that these enzymatic processes are linked and may be influenced simultaneously by the incubation conditions or substrate additions (Fig. 14B). There are also positive correlations between MBC and enzyme activities, especially AG activities. Some enzyme activities are negatively correlated with specific Soil C pools. PHD activity is strongly correlated to fPOC. A pronounced intensification in the correlation between total CO<sub>2</sub> concentration and microbial residue C is observed. Distinct correlations between SOM fractions and CO<sub>2</sub> concentration emerge, with fPOC displaying a positive correlation, while the correlation with MAOC is attenuated.

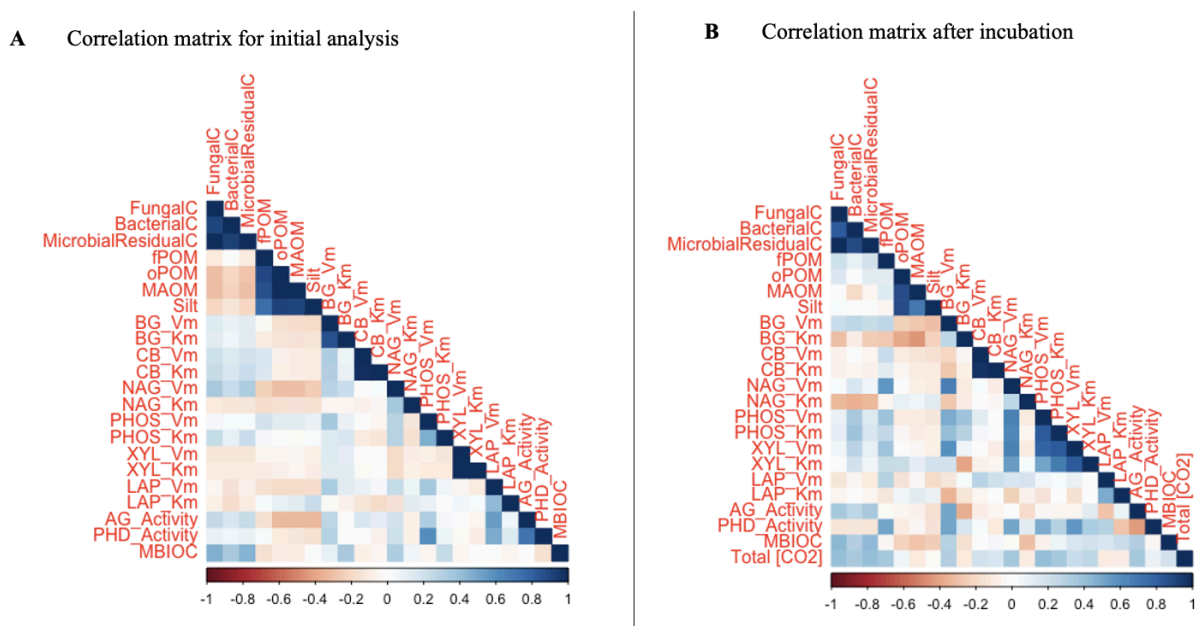


Fig. 14: Correlation matrix before (A) and after incubation (B). MBIOC refers to microbial biomass carbon (MBC).

#### 4. Discussion

Our findings underscore the nuanced response of soil C pools, such as POC and MAOC, to environmental stressors, aligning with findings that highlight the temperature sensitivity of soil C processes and their broader ecological feedback (Davidson and Janssens, 2006). Our analysis also sheds light on MBC variations in response to changing conditions, echoing Machmuller et al. (2016) emphasis on the significant role of seasonal dynamics over uniform temperature changes in influencing soil enzyme activities. By integrating these insights with enzyme activity data post-incubation, we contribute to an improved understanding of adaptive microbial strategies in the face of climate change, advocating for precise management strategies informed by the intricate relationships between microbial processes, soil C dynamics, and environmental factors.

#### *4.1. Substrate (C and nutrient) amendment but not temperature rise affects CO<sub>2</sub> mineralization*

The temporal and aggregate analyses of CO<sub>2</sub> mineralization under varying treatments and temperature conditions provide substantial insights into the complexities of soil C dynamics (Figs. 4&5). The data suggest that the addition of C, N, and P distinctly modulate the soil respiration process, a key component of the soil C cycle. No significant effect between the no amendment (None) and nutrient amendment (N+P) treatment was observed, which was the opposite of what we anticipated for nutrient-poor soils in our site. This may suggest that the microbial activity may have been constrained by factors other than nutrient availability, such as microbial community composition, the presence of inhibitory compounds, physical soil properties, rates of plant C inputs, or plant-microbe feedbacks (Davidson and Janssens, 2006; Mohan, 2019; Sihi et al., 2019). Additionally, the result could be inferred that this ecosystem is more constrained by C availability than by N and P, highlighting a C-limited system. This pattern resonates with ecological theories suggesting that microbial activity can be predominantly restricted by the scarcity of labile carbon, even more so than by other nutrients, thereby regulating the soil C cycle in a manner heavily dependent on C inputs (Davidson and Janssens, 2006; Sihi et al., 2019).

The temporal trend in Fig. 4 illustrated a clear response of soil microbial activities to nutrient and C additions, with the highest CO<sub>2</sub> flux observed in treatments where N+P+C were added. The sole addition of C (but not nutrients) and the combined addition of C and nutrients (N+P+C) increased respiration rates, which indicated that microbial activities were primarily limited by C substrates in our site, and when C-limitation was alleviated, microbial activities were limited by nutrients to meet their stoichiometric demands (Buchkowski et al., 2019). Our findings align

with the widely accepted view that microbial activity is spurred (or co-limited) by the availability of both C and nutrient substrates (Sihi et al., 2016; Malik et al., 2019; Domeignoz-Horta et al., 2023). The lack of significant interaction between treatment and temperature implied that while the availability of substrates is a fundamental driver of metabolic rates in our site, microbial response to temperature may remain relatively consistent under future warming as long as nutrient substrate availability remains constant, at least within the context of this study. If atmospheric N deposition were to increase in the Southeast, it could potentially alleviate the existing N-limitation in these soils. Consequently, this influx might shift the stoichiometric balance, possibly enhancing microbial activity and decomposition rates if C is simultaneously available. However, this shift could also lead to a saturation effect, where the excess nitrogen no longer serves as a limiting nutrient, potentially causing a cascade of ecological impacts such as changes in species composition, alterations in soil acidity, and disruptions in the existing microbial and plant community dynamics (Aber et al., 1989; Driscoll et al., 2003).

#### *4.2. Temperature but not treatment change affects SOC fractions*

Our study's findings concerning the differential responses of SOC fractions under various incubation conditions corroborate recent research suggesting that POC is more susceptible to environmental changes than MAOC, particularly fPOC (Rocci et al., 2021; Zhang et al., 2022). The limited proportion of fPOC in our samples suggests a general scarcity of readily available C substrates at our site. This observation aligns with the global synthesis by Rocci et al. (2021), which posits that POC serves as a sensitive indicator of SOC dynamics in response to global change factors. Our data reveal that oPOC, a specific sub-fraction of POC, was the predominant form across different temperature treatments both before and after incubation, as illustrated in

Fig. 6. The observed decline in oPOC under ambient temperatures post-incubation highlights POC's potential vulnerability to microbial decomposition even at moderate temperatures, echoed by Georgiou et al. (2022), which underscores POC's sensitivity to environmental variations. This decline also prompts speculation regarding the impact of lab handling and processing on soil aggregates. The observed decrease might not solely reflect the microbial decomposition processes but could also signal a disturbance-induced breakdown of soil aggregates, potentially altering the physical protection of oPOC and its availability to microbial activity. The labile nature of oPOC and its degradation can shed light on SOC stability in contrasting agricultural practices. No-till farming may bolster soil carbon stability by safeguarding soil aggregates and thus the encapsulated oPOC from microbial decay. In contrast, tilling breaks these aggregates, exposing oPOC to microbes and potentially hastening carbon turnover. Consequently, no-till practices may enhance soil carbon sequestration, as they help maintain higher stable SOC levels and influence microbial community dynamics critical for SOC stability (Six et al., 2002; Plaza-Bonilla et al., 2010).

The evident limitation of available (or labile) C substrates at our site is exacerbated by warming, leading to a reduction in fPOC with rising temperatures. This reduction could be attributed to an escalation in microbial activity at elevated temperatures, outpacing the fPOC pool's ability to meet the increased microbial demand. Consequently, we observed a form of thermal acclimation in microbial respiration, characterized by stable respiration rates at higher temperatures, indicative of a response to substrate limitation. The addition of labile C substrates led to an increase in microbial respiration, affirming the initial limitation by C availability. Moreover, when nutrients were supplemented alongside C, we observed enhanced microbial metabolism,

evidencing a co-limitation by both C and nutrient substrates at our site. This synergy between C and nutrient additions in stimulating microbial activity further supports the concept of co-limitation, emphasizing the critical interplay between C and nutrient availability (or ecological stoichiometry) in regulating soil microbial processes and SOC dynamics under changing environmental conditions (Sterner and Elser, 2002; Sihi et al., 2016; Malik et al., 2019; Domeignoz-Horta et al., 2023).

The observed decrease in fPOC with warming resonates with the emerging understanding that temperature-induced limitations on C substrates are likely driving soil CO<sub>2</sub> emission responses under warming conditions. Rocci et al. (2021) report a negative tendency of POC under warming, suggesting that increased temperatures may accelerate the microbial decomposition of POC, thereby reducing its stock in the soil. This is consistent with the concept that warmer temperatures enhance microbial activity, leading to a greater turnover of labile C pools like fPOC. The decrease in fPOC at elevated temperatures might, therefore, reflect a reduction in the availability of this labile C fraction. Critically, this trend underscores the concept of thermal acclimation (or apparent temperature sensitivity) of soil microbial respiration, primarily driven by the limitation of available or labile C substrates. As temperatures rise, microbial communities adjust their respiration rates in response to the availability of C substrates. This adaptive mechanism suggests that soil microbial respiration's temperature sensitivity is intricately linked to the dynamics of C substrate utilization. Under warming conditions, microbes increasingly rely on available labile C pools, such as fPOC, leading to a potential feedback loop where enhanced decomposition rates may reduce the soil's capacity to sequester C over time (Kirschbaum, 2013; Tucker et al., 2013; Pold et al., 2017; Hagerty et al., 2018; Domeignoz-Horta et al., 2023).

### *4.3. MBC responses to temperatures and treatments*

The response of MBC to soil incubation and various treatments presents intriguing insights into the microbial dynamics within soil ecosystems. The observed increase in MBC after incubation, particularly with C addition at temperatures of 26.5°C and 27.5°C (Fig. 7B), suggests a positive microbial response to added substrates, potentially indicating an enhanced microbial growth or a higher carbon use efficiency (CUE) under these conditions. The decrease in MBC with N+P and N+P+C treatments, irrespective of temperature, points to an intricate nutrient-microbial interaction where microbial efficiency may be altered, affecting both MBC and soil respiration rates (Malik et al., 2019; Chen et al., 2021). Within this context, Chen et al. (2021) found that nitrogen addition resulted in a decline in POC and MBC, attributing this to a shift in microbial physiology. Such shifts could translate into altered soil respiration rates, with potential implications for SOC turnover and stability, particularly in the POC fraction which is typically more labile and responsive to changes in microbial activity. The reduction in fPOC at elevated temperatures (Fig. 6), coupled with the increase in MBC, hints at a microbial community that is not only adapting but possibly also acclimating to warmer conditions by shifting its substrate utilization patterns (Bradford 2013; Crowther and Bradford, 2013; Davidson et al., 2014; Melillo et al., 2017; Sihi et al., 2018). Such shifts may involve breaking down more labile C pools, like fPOC, which is responsive to changes in microbial activity.

In addition, our observation that N+P treatments tend to have the lowest MBC aligns with insights from Lavallee et al. (2020), which suggest that microbial communities adapt their CUE in response to nutrient availability, thereby impacting SOC dynamics. The overall higher MBC

after incubation compared to pre-incubation levels across all treatments could indicate that the incubation conditions fostered microbial growth or activity and may be due to addition of substrates or breakdown of aggregates and release of otherwise occluded C or nutrients during soil processing (Fig. 7). This suggests a potential for increased microbial contribution to soil respiration (Figs. 4&5), which could amplify the release of CO<sub>2</sub> from soils, especially considering that soil respiration is a significant pathway for SOC loss. Despite the lack of statistical significance, which could be attributed to high intrinsic variability or potential limitations in experimental design, the trends observed in MBC and soil C fractions are revealing. The contrast observed between the effects of substrate additions on MBC versus SOC fractions points towards a potential decoupling between microbial growth and soil C storage. While substrate additions (N+P and N+P+C treatments) resulted in a decrease in MBC irrespective of temperature, this did not straightforwardly translate into increased C storage within any specific SOC fraction (Carey et al., 2016; Chen et al., 2021; Figs. 6&7). Instead, such nutrients and C may have influenced microbial communities to alter their resource allocation strategies—either favoring immediate growth over efficiency or adjusting their decomposition activities, which could affect the turnover rates of more stable C pools like oPOC. This possible decoupling underscores a complex scenario where microbial growth, spurred by nutrient availability, does not necessarily lead to enhanced soil C sequestration. Rather, it suggests that microbial communities might optimize their metabolic strategies under nutrient-rich conditions, potentially at the expense of C stabilization within the soil matrix (Carey et al., 2016; Malik et al., 2019; Chen et al., 2021).

#### *4.4. Microbial residual C responses to temperatures and treatments*

Microbial residual C, serving as a proxy for necromass, exhibited the greatest concentrations at 26.5°C before incubation, aligning with previous findings that moderate temperatures can enhance microbial metabolism, potentially leading to an accrual of necromass (Carey et al., 2016). However, the escalation of temperature to 27.5°C did not significantly augment the necromass, suggesting a threshold beyond which microbial mortality may not necessarily be temperature-driven (Machmuller et al., 2016, 2018, Fig. 8). In contrast to bacterial C, which displayed a robust presence and implied a higher turnover at all examined temperatures, fungal C demonstrated a more constant distribution across the thermal spectrum. This observation may infer relative stability in fungal C pools, potentially attributed to the resilient nature of fungal structures and the composition of fungal necromass that could be less susceptible to temperature-induced decay (Crowther et al., 2016, Figs. 8&9C). Our results echo with Wood et al. (2019) who noted the inherent stability of fungal-derived compounds in soil.

Interestingly, the N+P+C treatment consistently harbored higher microbial residual C after incubation, irrespective of the temperature variances (Fig. 9), which may reflect the co-limitation theory. The combined addition of C and nutrients in the N+P+C treatment could have synergistically enhanced microbial carbon use efficiency (CUE) and growth, leading to increased necromass production compared to samples without amendments, or those with only C or N+P additions. This interpretation is supported by the understanding that microbial communities can exhibit increased growth and CUE in response to balanced nutrient and C inputs, a concept partially supported by studies that have observed enhanced microbial activity with C and nutrient amendments (Sulman et al., 2014; Wieder et al., 2015). However, the lack of a pronounced difference between 25°C and 26.5°C after incubation suggests that microbial communities may

exhibit a degree of thermal acclimation to prevailing temperature (Bradford 2013; Crowther and Bradford, 2013; Davidson et al., 2014; Melillo et al., 2017; Sihi et al., 2018).

#### *4.5. Enzyme kinetics and activity response to treatments and temperatures*

The evaluation of enzymatic activities and kinetic parameters after 22 days of lab incubation revealed enzyme-specific responses to temperature treatments that have important implications for understanding soil C dynamics in response to climate change. The enzymes responsible for the degradation of labile C compounds, particularly CB, exhibited a clear temperature sensitivity, with a noticeable decline in  $V_{max}$  at the higher temperature of 27.5°C (Figs. 10B&12B), a trend not entirely aligned with enzyme denaturation at such moderate temperatures. This decrease in enzymatic efficiency, rather than being attributed to enzyme denaturation, might be associated with the production of different isoenzymes or alterations in the heat capacity of enzymes with warming, as proposed by Hobbs et al. (2013). The observed reduction in  $V_{max}$  of these enzymes at higher temperatures could also suggest a potential decline in the availability of labile C substrates (fPOC in our study, Fig. 6) under warming scenarios, potentially moderating the expected acceleration of C cycling predicted under climate warming (Davidson and Janssens, 2006; Sihi et al., 2019).

In contrast, enzymes targeted to N, such as LAP and NAG, maintained a consistent  $V_{max}$  across varied temperatures, suggesting a resilience of nitrogen-cycling processes to warming. This constancy in enzyme activity, alongside an unchanging  $K_m$ , indicates that the enzyme efficiency for these nitrogenous compounds does not alter with temperature increases, pointing towards a possible adaptive response to maintain nitrogen processing under warming scenarios (Sihi et al.,

2019; Tang et al., 2019, Figs. 10&12). The distinct response of PHD activity at 25°C, much higher than at other temperatures and compared to AG, may reflect the inherent P limitation characteristic of subtropical soils (Sihi et al., 2019; Figs. 11B&13B-D). This aligns with the understanding that P-limitation can significantly influence soil organic C turnover in subtropical soils and is a critical factor in ecosystem responses to climate change (Alster et al., 2016; Carey et al., 2016; Sihi et al., 2019; Tang et al., 2019). The highest V<sub>max</sub> for BG under the N+P+C treatment at 27.5°C, as opposed to 26.5°C, juxtaposed with the decrease in V<sub>max</sub> due to simple C addition, provides an intriguing insight into how combined C and nutrient amendments may differentially influence enzyme activities and, in turn, SOM fractions (Figs. 6&12A). This suggests a complex interplay between enzyme kinetics and SOM fractions under warming conditions, potentially linked to the co-limitation theory previously discussed in the context of CO<sub>2</sub> flux results.

#### *4.6. Correlations matrix interpretations*

The initial state of soil prior to incubation presents a complex matrix of interrelationships among microbial communities, SOM fractions, and enzyme activities. The weakened correlation coefficients observed in Fig. 14A reflect a natural ecosystem where interdependencies among soil biotic and abiotic factors are less distinct. This is evident in the nuanced associations between MBC, fungal C, and microbial residue C, which are more pronounced than those with bacterial C. These findings could imply a differential role of fungal and bacterial communities in the dynamics of soil C pool under ambient conditions.

The intensified post-incubation correlations suggest a more dynamic soil environment where increased MBC could potentially stimulate necromass formation (Fig. 14B). This premise is supported by the enhanced correlations between MBC and enzyme activities post-incubation, reflecting a surge in microbial metabolism. The corresponding increase in total CO<sub>2</sub> concentrations could be attributed to both the direct respiration of the expanded microbial population and the decomposition of increased necromass, a byproduct of microbial turnover. The rise in fPOC alongside increased total CO<sub>2</sub> concentrations points towards a rapid turnover of this labile organic C fraction. The incubation conditions seem to accelerate the microbial processing of fPOC, as evidenced by the strong enzymatic activity. Conversely, the stable or decreased levels of MAOC suggest that this more recalcitrant fraction is less impacted by microbial action, possibly due to its inherent resistance to enzymatic breakdown or its protection within the soil matrix.

To explain CO<sub>2</sub> production from an enzymatic perspective, we consider enzyme kinetics. Post-incubation, increased V<sub>max</sub> for enzymes like BG, CB, and NAG signifies an elevated enzymatic capacity for catalyzing the transformation of soil organic compounds. This escalation in enzyme activity implies that the substrates for these enzymes, predominantly found in the fPOC fraction, are being decomposed more efficiently, resulting in increased CO<sub>2</sub> evolution as a metabolic byproduct. This post-incubation scenario presents a soil system where microbial activity, and thus enzymatic processes, are no longer operating in isolation but are part of an integrated network. The enzymes, catalyzing the conversion of organic material into microbial biomass, could, in turn, be contributing to the formation of necromass as microbial cells die and lyse, thereby perpetuating the cycle of SOM transformation.

The observed data postulate a reinforcing feedback mechanism where enhanced microbial biomass results in a spike in enzyme-mediated decomposition processes, further accelerating the cycle of C through various pools in the soil. This mechanism aligns with our understanding of the soil C cycle, where the breakdown of organic matter by microbial action is a critical pathway for CO<sub>2</sub> production in terrestrial ecosystems.

## 5. Conclusions and Future Implications

In summary, our exploration into the dynamics of the soil carbon cycle in the face of climate change uncovers a nuanced and evolving relationship among microbial activities, carbon storage within the soil, and shifts in environmental conditions. Our research sheds light on the capacity of microbial communities to adapt to fluctuations in temperature, pointing to possible resilience strategies that may affect the accumulation and decomposition of soil carbon. This study underlines the imperative for ongoing investigation into the regulatory mechanisms of soil carbon dynamics and how microbial entities adapt to environmental transformations.

Our results underscore the profound influence that alterations in substrates (C and nutrients) and temperature have on the process of soil organic carbon loss (CO<sub>2</sub> mineralization) or stabilization, highlighting the pivotal function of microbial actions in regulating the movement of C through soil systems. Enhanced CO<sub>2</sub> mineralization under C and nutrient additions across all temperature conditions underscores the importance of substrate availability in stimulating microbial activity and soil C cycling. Our results illustrate the co-limitation by C and nutrients, with the most significant CO<sub>2</sub> flux observed under combined carbon and nutrient additions (N+P+C). The POC, especially the fPOC, exhibited higher sensitivity to temperature changes compared to

MAOC. This sensitivity, coupled with the observed decline in fPOC at elevated temperatures, signals potential vulnerability to microbial decomposition under warming scenarios and underscores the dynamic nature of SOC components in response to climatic alterations. The observed increase in MBC with substrate additions at warmer temperatures indicates a positive microbial response to added substrates, suggesting enhanced microbial growth or CUE. Conversely, the decrease in MBC with N+P+C treatments, irrespective of temperature, points to complex interactions between substrates and microbial communities that may influence SOC turnover and stability. The consistent increase in microbial residual carbon under the N+P+C treatment across various temperatures supports the theory of microbial co-limitation and underscores the synergistic effects of combined nutrients and carbon amendments on microbial necromass production. Additionally, the nuanced responses of enzyme activities to temperature and substrate treatments provide critical insights into the adaptive strategies of soil microbial communities in the face of changing environmental conditions.

However, due to limited soil samples, we did not perform additional analyses and test other environmental factors. For future studies, microbial carbon use efficiency (CUE) and microbial community analysis (functional genes, metagenomics, or metatranscriptomics) should be done to further improve our understanding of the hidden mechanisms of soil C cycle. Other environmental factors such as soil moisture content can be added to represent widely-observed warming-induced drought events. Additionally, we did not look into the effects of different canopy covers and their interactions with warming on different soil C pools in this study, which future research can investigate further. We did not monitor the potential changes in soil pH and bulk density over time. Future research can take these factors into account. For our study, the incubation length was 22 days. Future studies can focus on a more long-term incubation to

clearly observe the changes over time. Enhancing our grasp on these intricate interconnections lays the groundwork for devising more effective strategies for conservation and management, safeguarding the integrity of soil resources and their indispensable function within the global carbon framework.

## 6. References

- Aber, J.D., Nadelhoffer, K.J., Steudler, P., Melillo, J.M., 1989. Nitrogen Saturation in Northern Forest Ecosystems. *BioScience* 39, 378–386. <https://doi.org/10.2307/1311067>
- Allison, S.D., Wallenstein, M.D., Bradford, M.A., 2010. Soil-carbon response to warming dependent on microbial physiology. *Nat. Geosci.* 3, 336–340. <https://doi.org/10.1038/ngeo846>
- Alster, C.J., Baas, P., Wallenstein, M.D., Johnson, N.G., von Fischer, J.C., 2016. Temperature Sensitivity as a Microbial Trait Using Parameters from Macromolecular Rate Theory. *Front. Microbiol.* 7. <https://doi.org/10.3389/fmicb.2016.01821>
- Beck, T., Joergensen, R.G., Kandeler, E., Makeschin, F., Nuss, E., Oberholzer, H.R., Scheu, S., 1997. An inter-laboratory comparison of ten different ways of measuring soil microbial biomass C. *Soil Biol. Biochem.* 29, 1023–1032. [https://doi.org/10.1016/S0038-0717\(97\)00030-8](https://doi.org/10.1016/S0038-0717(97)00030-8)
- Bell, C.W., Fricks, B.E., Rocca, J.D., Steinweg, J.M., McMahon, S.K., Wallenstein, M.D., 2013. High-throughput Fluorometric Measurement of Potential Soil Extracellular Enzyme Activities. *J. Vis. Exp.* 50961. <https://doi.org/10.3791/50961>
- Blagodatskaya, E., Blagodatsky, S., Khomyakov, N., Myachina, O., Kuzyakov, Y., 2016. Temperature sensitivity and enzymatic mechanisms of soil organic matter decomposition along an altitudinal gradient on Mount Kilimanjaro. *Sci. Rep.* 6, 22240.

<https://doi.org/10.1038/srep22240>

- Bradford, M.A., 2013. Thermal adaptation of decomposer communities in warming soils. *Front. Microbiol.* 4. <https://doi.org/10.3389/fmicb.2013.00333>
- Buchkowski, R.W., Shaw, A.N., Sihi, D., Smith, G.R., Keiser, A.D., 2019. Constraining Carbon and Nutrient Flows in Soil With Ecological Stoichiometry. *Front. Ecol. Evol.* 7, 382. <https://doi.org/10.3389/fevo.2019.00382>
- Buckeridge, K.M., Creamer, C., Whitaker, J., 2022. Deconstructing the microbial necromass continuum to inform soil carbon sequestration. *Funct. Ecol.* 36, 1396–1410. <https://doi.org/10.1111/1365-2435.14014>
- Burns, R.G., DeForest, J.L., Marxsen, J., Sinsabaugh, R.L., Stromberger, M.E., Wallenstein, M.D., Weintraub, M.N., Zoppini, A., 2013. Soil enzymes in a changing environment: Current knowledge and future directions. *Soil Biol. Biochem.* 58, 216–234. <https://doi.org/10.1016/j.soilbio.2012.11.009>
- Carey, J.C., Tang, J., Templer, P.H., Kroeger, K.D., Crowther, T.W., Burton, A.J., Dukes, J.S., Emmett, B., Frey, S.D., Heskell, M.A., Jiang, L., Machmuller, M.B., Mohan, J., Panetta, A.M., Reich, P.B., Reinsch, S., Wang, X., Allison, S.D., Bamminger, C., Bridgham, S., Collins, S.L., de Dato, G., Eddy, W.C., Enquist, B.J., Estiarte, M., Harte, J., Henderson, A., Johnson, B.R., Larsen, K.S., Luo, Y., Marhan, S., Melillo, J.M., Peñuelas, J., Pfeifer-Meister, L., Poll, C., Rastetter, E., Reinmann, A.B., Reynolds, L.L., Schmidt, I.K., Shaver, G.R., Strong, A.L., Suseela, V., Tietema, A., 2016. Temperature response of soil respiration largely unaltered with experimental warming. *Proc. Natl. Acad. Sci.* 113, 13797–13802. <https://doi.org/10.1073/pnas.1605365113>
- Chen, Y., Liu, X., Hou, Y., Zhou, S., Zhu, B., 2021. Particulate organic carbon is more vulnerable

to nitrogen addition than mineral-associated organic carbon in soil of an alpine meadow.

Plant Soil 458, 93–103. <https://doi.org/10.1007/s11104-019-04279-4>

Cotrufo, M.F., Wallenstein, M.D., Boot, C.M., Deneff, K., Paul, E., 2013. The Microbial Efficiency-Matrix Stabilization (MEMS) framework integrates plant litter decomposition with soil organic matter stabilization: do labile plant inputs form stable soil organic matter? Glob. Change Biol. 19, 988–995. <https://doi.org/10.1111/gcb.12113>

Crowther, T.W., Bradford, M.A., 2013. Thermal acclimation in widespread heterotrophic soil microbes. Ecol. Lett. 16, 469–477. <https://doi.org/10.1111/ele.12069>

Crowther, T.W., Todd-Brown, K.E.O., Rowe, C.W., Wieder, W.R., Carey, J.C., Machmuller, M.B., Snoek, B.L., Fang, S., Zhou, G., Allison, S.D., Blair, J.M., Bridgham, S.D., Burton, A.J., Carrillo, Y., Reich, P.B., Clark, J.S., Classen, A.T., Dijkstra, F.A., Elberling, B., Emmett, B.A., Estiarte, M., Frey, S.D., Guo, J., Harte, J., Jiang, L., Johnson, B.R., Kröel-Dulay, G., Larsen, K.S., Laudon, H., Lavalley, J.M., Luo, Y., Lupascu, M., Ma, L.N., Marhan, S., Michelsen, A., Mohan, J., Niu, S., Pendall, E., Peñuelas, J., Pfeifer-Meister, L., Poll, C., Reinsch, S., Reynolds, L.L., Schmidt, I.K., Sistla, S., Sokol, N.W., Templer, P.H., Treseder, K.K., Welker, J.M., Bradford, M.A., 2016. Quantifying global soil carbon losses in response to warming. Nature 540, 104–108.

<https://doi.org/10.1038/nature20150>

Dash, P.K., Bhattacharyya, P., Roy, K.S., Neogi, S., Nayak, A.K., 2019. Environmental constraints' sensitivity of soil organic carbon decomposition to temperature, management practices and climate change. Ecol. Indic. 107, 105644.

<https://doi.org/10.1016/j.ecolind.2019.105644>

- Davidson, E.A., 2020. Carbon loss from tropical soils increases on warming. *Nature* 584, 198–199.
- Davidson, E.A., Janssens, I.A., 2006. Temperature sensitivity of soil carbon decomposition and feedbacks to climate change. *Nature* 440, 165–173. <https://doi.org/10.1038/nature04514>
- Davidson, E.A., Savage, K.E., Finzi, A.C., 2014. A big-microsite framework for soil carbon modeling. *Glob. Change Biol.* 20, 3610–3620. <https://doi.org/10.1111/gcb.12718>
- Driscoll, C.T., Lawrence, G.B., Bulger, A.J., Butler, T.J., Cronan, C.S., Eagar, C., Lambert, K.F., Likens, G.E., Stoddard, J.L., Weathers, K.C., 2001. Acidic Deposition in the Northeastern United States: Sources and Inputs, Ecosystem Effects, and Management Strategies. *BioScience* 51, 180.
- Domeignoz-Horta, L.A., Pold, G., Erb, H., Sebag, D., Verrecchia, E., Northen, T., Louie, K., Eloë-Fadrosch, E., Pennacchio, C., Knorr, M.A., Frey, S.D., Melillo, J.M., DeAngelis, K.M., 2023. Substrate availability and not thermal acclimation controls microbial temperature sensitivity response to long-term warming. *Glob. Change Biol.* 29, 1574–1590. <https://doi.org/10.1111/gcb.16544>
- Falloon, P., Jones, C.D., Ades, M., Paul, K., 2011. Direct soil moisture controls of future global soil carbon changes: An important source of uncertainty: SOIL MOISTURE AND SOIL CARBON. *Glob. Biogeochem. Cycles* 25, n/a-n/a. <https://doi.org/10.1029/2010GB003938>
- Fanin, N., Mooshammer, M., Sauvadet, M., Meng, C., Alvarez, G., Bernard, L., Bertrand, I., Blagodatskaya, E., Bon, L., Fontaine, S., Niu, S., Lashermes, G., Maxwell, T.L., Weintraub, M.N., Wingate, L., Moorhead, D., Nottingham, A.T., 2022. Soil enzymes in response to climate warming: Mechanisms and feedbacks. *Funct. Ecol.* 36, 1378–1395.

<https://doi.org/10.1111/1365-2435.14027>

Georgiou, K., Jackson, R.B., Vindušková, O., Abramoff, R.Z., Ahlström, A., Feng, W., Harden, J.W., Pellegrini, A.F.A., Polley, H.W., Soong, J.L., Riley, W.J., Torn, M.S., 2022. Global stocks and capacity of mineral-associated soil organic carbon. *Nat. Commun.* 13, 3797.

<https://doi.org/10.1038/s41467-022-31540-9>

German, D.P., Weintraub, M.N., Grandy, A.S., Lauber, C.L., Rinkes, Z.L., Allison, S.D., 2011. Optimization of hydrolytic and oxidative enzyme methods for ecosystem studies. *Soil Biol. Biochem.* 43, 1387–1397. <https://doi.org/10.1016/j.soilbio.2011.03.017>

Gross, C.D., Harrison, R.B., 2019. The Case for Digging Deeper: Soil Organic Carbon Storage, Dynamics, and Controls in Our Changing World. *Soil Syst.* 3, 28.

<https://doi.org/10.3390/soilsystems3020028>

Hagerty, S.B., Allison, S.D., Schimel, J.P., 2018. Evaluating soil microbial carbon use efficiency explicitly as a function of cellular processes: implications for measurements and models. *Biogeochemistry* 140, 269–283. <https://doi.org/10.1007/s10533-018-0489-z>

Haney, R.L., Haney, E.B., Smith, D.R., Harmel, R.D., White, M.J., 2018. The soil health tool—Theory and initial broad-scale application. *Appl. Soil Ecol.* 125, 162–168.

<https://doi.org/10.1016/j.apsoil.2017.07.035>

Hobbs, J.K., Jiao, W., Easter, A.D., Parker, E.J., Schipper, L.A., Arcus, V.L., 2013. Change in Heat Capacity for Enzyme Catalysis Determines Temperature Dependence of Enzyme Catalyzed Rates. *ACS Chem. Biol.* 8, 2388–2393. <https://doi.org/10.1021/cb4005029>

Indorf, C., Dyckmans, J., Khan, K.S., Joergensen, R.G., 2011. Optimisation of amino sugar quantification by HPLC in soil and plant hydrolysates. *Biol. Fertil. Soils* 47, 387–396.

<https://doi.org/10.1007/s00374-011-0545-5>

- Ito A, Wagai R (2017) Global distribution of clay-size minerals on land surface for biogeochemical and climatological studies. *Sci Data* 4:170103
- Jilling, A., Kane, D., Williams, A., Yannarell, A.C., Davis, A., Jordan, N.R., Koide, R.T., Mortensen, D.A., Smith, R.G., Snapp, S.S., Spokas, K.A., Stuart Grandy, A., 2020. Rapid and distinct responses of particulate and mineral-associated organic nitrogen to conservation tillage and cover crops. *Geoderma* 359, 114001. <https://doi.org/10.1016/j.geoderma.2019.114001>
- Jilling, A., Keiluweit, M., Contosta, A.R., Frey, S., Schimel, J., Schnecker, J., Smith, R.G., Tiemann, L., Grandy, A.S., 2018. Minerals in the rhizosphere: overlooked mediators of soil nitrogen availability to plants and microbes. *Biogeochemistry* 139, 103–122. <https://doi.org/10.1007/s10533-018-0459-5>
- Joergensen, R.G., 2018. Amino sugars as specific indices for fungal and bacterial residues in soil. *Biol. Fertil. Soils* 54, 559–568. <https://doi.org/10.1007/s00374-018-1288-3>
- Kirschbaum, M.U.F., 2013. Seasonal variations in the availability of labile substrate confound the temperature dependence of organic matter decomposition. *Soil Biol. Biochem.* 57, 568–576. <https://doi.org/10.1016/j.soilbio.2012.10.012>
- Kuzyakov, Y., Dijkstra, P., n.d. Carbon Use Efficiency: Universal approach to link microbial growth, death, turnover and maintenance in steady state ecosystems.
- Lavallee, J.M., Soong, J.L., Cotrufo, M.F., 2020. Conceptualizing soil organic matter into particulate and mineral-associated forms to address global change in the 21st century. *Glob. Change Biol.* 26, 261–273. <https://doi.org/10.1111/gcb.14859>
- Li, D., Zheng, B., Chu, Z., Liu, Y., Huang, M., 2019. Seasonal variations of performance and operation in field-scale storing multipond constructed wetlands for nonpoint source

- pollution mitigation in a plateau lake basin. *Bioresour. Technol.* 280, 295–302.  
<https://doi.org/10.1016/j.biortech.2019.01.116>
- Li, J., Wang, G., Allison, S.D., Mayes, M.A., Luo, Y., 2014. Soil carbon sensitivity to temperature and carbon use efficiency compared across microbial-ecosystem models of varying complexity. *Biogeochemistry* 119, 67–84.  
<https://doi.org/10.1007/s10533-013-9948-8>
- Liang, C., Amelung, W., Lehmann, J., Kästner, M., 2019. Quantitative assessment of microbial necromass contribution to soil organic matter. *Glob. Change Biol.* 25, 3578–3590.  
<https://doi.org/10.1111/gcb.14781>
- Ma, X., Razavi, B.S., Holz, M., Blagodatskaya, E., Kuzyakov, Y., 2017. Warming increases hotspot areas of enzyme activity and shortens the duration of hot moments in the root-detritusphere. *Soil Biol. Biochem.* 107, 226–233.  
<https://doi.org/10.1016/j.soilbio.2017.01.009>
- Machmuller, M.B., Ballantyne, F., Markewitz, D., Thompson, A., Wurzbürger, N., Frankson, P.T., Mohan, J.E., 2018. Temperature sensitivity of soil respiration in a low-latitude forest ecosystem varies by season and habitat but is unaffected by experimental warming. *Biogeochemistry* 141, 63–73. <https://doi.org/10.1007/s10533-018-0501-7>
- Machmuller, M.B., Mohan, J.E., Minucci, J.M., Phillips, C.A., Wurzbürger, N., 2016. Season, but not experimental warming, affects the activity and temperature sensitivity of extracellular enzymes. *Biogeochemistry* 131, 255–265.  
<https://doi.org/10.1007/s10533-016-0277-6>
- Mohan, J.E., Wadgymar, S.M., Winkler, D.E., Anderson, J.T., Frankson, P.T., Hannifin, R., Benavides, K., Kueppers, L.M., Melillo, J.M., 2019. Plant reproductive fitness and

- phenology responses to climate warming: Results from native populations, communities, and ecosystems, in: *Ecosystem Consequences of Soil Warming*. Elsevier, pp. 61–102.  
<https://doi.org/10.1016/B978-0-12-813493-1.00004-1>
- Malik, A.A., Puissant, J., Goodall, T., Allison, S.D., Griffiths, R.I., 2019. Soil microbial communities with greater investment in resource acquisition have lower growth yield. *Soil Biol. Biochem.* 132, 36–39. <https://doi.org/10.1016/j.soilbio.2019.01.025>
- Melillo, J.M., Frey, S.D., DeAngelis, K.M., Werner, W.J., Bernard, M.J., Bowles, F.P., Pold, G., Knorr, M.A., Grandy, A.S., 2017. Long-term pattern and magnitude of soil carbon feedback to the climate system in a warming world. *Science* 358, 101–105.  
<https://doi.org/10.1126/science.aan2874>
- Moyano, F.E., Vasilyeva, N., Menichetti, L., 2018. Diffusion limitations and Michaelis–Menten kinetics as drivers of combined temperature and moisture effects on carbon fluxes of mineral soils. *Biogeosciences* 15, 5031–5045. <https://doi.org/10.5194/bg-15-5031-2018>
- NOAA (2024) National oceanic and atmospheric administration. National climate data center, Athens, Georgia, Ben Epps Airport Climate Station
- Nocita, M., Stevens, A., Noon, C., van Wesemael, B., 2013. Prediction of soil organic carbon for different levels of soil moisture using Vis-NIR spectroscopy. *Geoderma* 199, 37–42.  
<https://doi.org/10.1016/j.geoderma.2012.07.020>
- Nottingham, A.T., Gloor, E., Bååth, E., Meir, P., 2022. Soil carbon and microbes in the warming tropics. *Funct. Ecol.* 36, 1338–1354. <https://doi.org/10.1111/1365-2435.14050>
- Nottingham, A.T., Meir, P., Velasquez, E., Turner, B.L., 2020. Soil carbon loss by experimental warming in a tropical forest. *Nature* 584, 234–237.  
<https://doi.org/10.1038/s41586-020-2566-4>

- Pellegrini, A.F.A., Reich, P.B., Hobbie, S.E., Coetsee, C., Wigley, B., February, E., Georgiou, K., Terrer, C., Brookshire, E.N.J., Ahlström, A., Nieradzik, L., Sitch, S., Melton, J.R., Forrest, M., Li, F., Hantson, S., Burton, C., Yue, C., Ciais, P., Jackson, R.B., 2023. Soil carbon storage capacity of drylands under altered fire regimes. *Nat. Clim. Change* 13, 1089–1094. <https://doi.org/10.1038/s41558-023-01800-7>
- Pierson, D., Evans, L., Kayhani, K., Bowden, R.D., Nadelhoffer, K., Simpson, M., Lajtha, K., 2021. Mineral stabilization of soil carbon is suppressed by live roots, outweighing influences from litter quality or quantity. *Biogeochemistry* 154, 433–449. <https://doi.org/10.1007/s10533-021-00804-9>
- Plaza-Bonilla, D., Cantero-Martínez, C., Álvaro-Fuentes, J., 2010. Tillage effects on soil aggregation and soil organic carbon profile distribution under Mediterranean semi-arid conditions: Tillage effects on soil aggregation and soil organic carbon distribution. *Soil Use Manag.* 26, 465–474. <https://doi.org/10.1111/j.1475-2743.2010.00298.x>
- Pold, G., Grandy, A.S., Melillo, J.M., DeAngelis, K.M., 2017. Changes in substrate availability drive carbon cycle response to chronic warming. *Soil Biol. Biochem.* 110, 68–78. <https://doi.org/10.1016/j.soilbio.2017.03.002>
- Reynolds, S.G., 1970. The gravimetric method of soil moisture determination. *Journal of Hydrology* 11. 258-273.
- Rocci, K.S., Lavalley, J.M., Stewart, C.E., Cotrufo, M.F., 2021. Soil organic carbon response to global environmental change depends on its distribution between mineral-associated and particulate organic matter: A meta-analysis. *Sci. Total Environ.* 793, 148569. <https://doi.org/10.1016/j.scitotenv.2021.148569>
- Schipper, L.A., Hobbs, J.K., Rutledge, S., Arcus, V.L., 2014. Thermodynamic theory explains

- the temperature optima of soil microbial processes and high  $Q_{10}$  values at low temperatures. *Glob. Change Biol.* 20, 3578–3586. <https://doi.org/10.1111/gcb.12596>
- Sihi, D., Inglett, P.W., Gerber, S., Inglett, K.S., 2018. Rate of warming affects temperature sensitivity of anaerobic peat decomposition and greenhouse gas production. *Glob. Change Biol.* 24. <https://doi.org/10.1111/gcb.13839>
- Sihi, D., Inglett, P.W., Inglett, K.S., 2019. Warming rate drives microbial nutrient demand and enzyme expression during peat decomposition. *Geoderma* 336, 12–21. <https://doi.org/10.1016/j.geoderma.2018.08.027>
- Six, J., Feller, C., Denef, K., Ogle, S.M., De Moraes, J.C., Albrecht, A., 2002. Soil organic matter, biota and aggregation in temperate and tropical soils - Effects of no-tillage. *Agronomie* 22, 755–775. <https://doi.org/10.1051/agro:2002043>
- Staudinger, J., Roberts, P.V., 1996. A critical review of Henry's law constants for environmental applications. *Crit. Rev. Environ. Sci. Technol.* 26, 205–297. <https://doi.org/10.1080/10643389609388492>
- Sterner, W., Robert, and James J. Elser. *Ecological stoichiometry: the biology of elements from molecules to the biosphere*. Princeton UP, 2002, [press.princeton.edu/books/paperback/9780691074917/ecological-stoichiometry](http://press.princeton.edu/books/paperback/9780691074917/ecological-stoichiometry).
- Sulman, B.N., Phillips, R.P., Oishi, A.C., Shevliakova, E., Pacala, S.W., 2014. Microbe-driven turnover offsets mineral-mediated storage of soil carbon under elevated CO<sub>2</sub>. *Nat. Clim. Change* 4, 1099–1102. <https://doi.org/10.1038/nclimate2436>
- Spohn, M., Klaus, K., Wanek, W., Richter, A., 2016. Microbial carbon use efficiency and biomass turnover times depending on soil depth – Implications for carbon cycling. *Soil Biol. Biochem.* 96, 74–81. <https://doi.org/10.1016/j.soilbio.2016.01.016>

- Tang, J., Bradford, M.A., Carey, J., Crowther, T.W., Machmuller, M.B., Mohan, J.E., Todd-Brown, K., 2019. Temperature sensitivity of soil carbon, in: *Ecosystem Consequences of Soil Warming*. Elsevier, pp. 175–208.  
<https://doi.org/10.1016/B978-0-12-813493-1.00009-0>
- Tucker, C.L., Bell, J., Pendall, E., Ogle, K., 2013. Does declining carbon-use efficiency explain thermal acclimation of soil respiration with warming? *Glob. Change Biol.* 19, 252–263.  
<https://doi.org/10.1111/gcb.12036>
- Vaughn, L.J.S., Torn, M.S., 2019. <sup>14</sup>C evidence that millennial and fast-cycling soil carbon are equally sensitive to warming. *Nat. Clim. Change* 9, 467–471.  
<https://doi.org/10.1038/s41558-019-0468-y>
- Wang, G., Post, W.M., Mayes, M.A., 2013. Development of microbial-enzyme-mediated decomposition model parameters through steady-state and dynamic analyses. *Ecol. Appl.* 23, 255–272. <https://doi.org/10.1890/12-0681.1>
- Wei, H., Guenet, B., Vicca, S., Nunan, N., AbdElgawad, H., Pouteau, V., Shen, W., Janssens, I.A., 2014. Thermal acclimation of organic matter decomposition in an artificial forest soil is related to shifts in microbial community structure. *Soil Biol. Biochem.* 71, 1–12.  
<https://doi.org/10.1016/j.soilbio.2014.01.003>
- Wickham H, Vaughan D, Girlich M (2024). *tidyr: Tidy Messy Data*. R package version 1.3.1, <https://github.com/tidyverse/tidyr>, <https://tidyr.tidyverse.org>.
- Wickham H, François R, Henry L, Müller K, Vaughan D (2023). *dplyr: A Grammar of Data Manipulation*. R package version 1.1.4, <https://github.com/tidyverse/dplyr>, <https://dplyr.tidyverse.org>.

- Wickham H (2023). stringr: Simple, Consistent Wrappers for Common String Operations. R package version 1.5.1, <https://github.com/tidyverse/stringr>, <https://stringr.tidyverse.org>.
- Wickham, H. (2016). *Ggplot2: Elegant graphics for data analysis* (2nd ed.) [PDF]. Springer International Publishing.
- Wieder, W.R., Grandy, A.S., Kallenbach, C.M., Taylor, P.G., Bonan, G.B., 2015. Representing life in the Earth system with soil microbial functional traits in the MIMICS model (preprint). Biogeosciences. <https://doi.org/10.5194/gmdd-8-2011-2015>
- Wood, T.E., Cavaleri, M.A., Giardina, C.P., Khan, S., Mohan, J.E., Nottingham, A.T., Reed, S.C., Slot, M., 2019. Soil warming effects on tropical forests with highly weathered soils, in: *Ecosystem Consequences of Soil Warming*. Elsevier, pp. 385–439. <https://doi.org/10.1016/B978-0-12-813493-1.00015-6>
- Woody, A.I., 2013. How is the Ideal Gas Law Explanatory? *Sci. Educ.* 22, 1563–1580. <https://doi.org/10.1007/s11191-011-9424-6>
- Xu, X., Shi, Z., Li, D., Rey, A., Ruan, H., Craine, J.M., Liang, J., Zhou, J., Luo, Y., 2016. Soil properties control decomposition of soil organic carbon: Results from data-assimilation analysis. *Geoderma* 262, 235–242. <https://doi.org/10.1016/j.geoderma.2015.08.038>
- Zhang, F., Chen, X., Yao, S., Ye, Y., Zhang, B., 2022. Responses of soil mineral-associated and particulate organic carbon to carbon input: A meta-analysis. *Sci. Total Environ.* 829, 154626. <https://doi.org/10.1016/j.scitotenv.2022.154626>

## 7. Appendix

Table 1: p-values for **initial** analyses in terms of temperatures from ANOVA.

	fPOC	oPOC	coarse MAOC	fine MAOC	MBC	MRC	Fungal C	Bacterial C	BG Vmax	BG Km	CB Vmax	CB Km	XYL Vmax	XYL Km	LAP Vmax	LAP Km	NAG Vmax	NAG Km	PHOS Vmax	PHOS Km	PHD Activity	AG Activity
P values	0.43	0.44	0.35	0.22	0.44	0.37	0.38	0.39	0.081	0.25	0.30	0.12	0.49	0.50	0.023*	0.86	0.94	0.27	0.277	0.78	0.006**	0.018*

Symbols:  $p < 0.0001$  “\*\*\*\*”,  $p < 0.001$  “\*\*\*”,  $p < 0.01$  “\*\*”,  $p < 0.1$  “\*”. fPOC stands for free particulate organic carbon; oPOC stands for occlude particulate organic carbon; MAOC stands for mineral-associated organic carbon; MBC stands for microbial biomass C; MRC stands for microbial residual C.

Table 2: p-values for **post-incubation** analyses in terms of **treatments** from ANOVA.

	CO <sub>2</sub> Mineralization	Total CO <sub>2</sub>	fPOC	oPOC	coarse MAOC	fine MAOC	MBC	MRC	Fungal C	Bacteri al C	BG Vmax	BG Km	CB Vmax	CB Km	XYL Vmax	XYL Km	LAP Vmax	LAP Km	NAG Vmax	NAG Km	PHOS Vmax	PHOS Km	AG Activity	PHD Activity
P values	<2e-16** *	5.91e-07**	0.45	0.99	0.87	0.97	0.34	0.24	0.31	0.10	0.0144*	0.88	0.43	0.36	0.28	0.47	0.29	0.76	0.006*	0.56	0.0006** *	0.022*	0.007**	0.32

Symbols:  $p < 0.0001$  “\*\*\*\*”,  $p < 0.001$  “\*\*\*”,  $p < 0.01$  “\*\*”,  $p < 0.1$  “\*.”

Table 3: p-values for **post-incubation** analyses in terms of **temperatures** from ANOVA.

	CO <sub>2</sub> Mineralization	Total CO <sub>2</sub>	fPOC	oPOC	coarse MAOC	fine MAOC	MB C	MRC	Fungal C	Bacter ial C	BG Vmax	BG Km	CB Vmax	CB Km	XYL Vmax	XYL Km	LAP Vmax	LAP Km	NAG Vmax	NAG Km	PHOS Vmax	PHOS Km	AG Activity	PHD Activity
P values	0.49	0.65	0.026 *	0.05	0.13	0.064	0.42	0.044	0.038*	0.13	0.90	0.0002* **	0.66	0.58	0.079	0.31	0.043*	0.37	0.002* *	0.46	0.004* *	0.29	0.0007* **	2.16e-13* **

Symbols:  $p < 0.0001$  “\*\*\*\*”,  $p < 0.001$  “\*\*\*”,  $p < 0.01$  “\*\*”,  $p < 0.1$  “\*.”

Table 4: p-values for **post-incubation** analyses in terms of **treatments : temperatures** from ANOVA.

	CO <sub>2</sub> Mineralization	Total CO <sub>2</sub>	fPOC	oPOC	coarse MAOC	fine MAOC	MBC	MRC	Fungal C	Bacterial C	BG Vmax	BG Km	CB Vmax	CB Km	XYL Vmax	XYL Km	LAP Vmax	LAP Km	NAG Vmax	NAG Km	PHOS Vmax	PHOS Km	AG Activity	PHD Activity
P values	0.69	0.89	0.48	0.99	0.94	0.83	0.89	0.94	0.97	0.38	0.37	0.12	0.73	0.67	0.93	0.99	0.78	0.59	0.20	0.49	0.23	0.57	0.05	0.34

Symbols:  $p < 0.0001$  “\*\*\*\*”,  $p < 0.001$  “\*\*\*”,  $p < 0.01$  “\*\*”,  $p < 0.1$  “\*.”

Table 5: Detailed information for the field plots in Whitehall Forest, Athens, GA. NCC stands for non-chamber control, indicating no greenhouse plastic around the plot or buried soil warming cables, and the plots are surrounded by chickenwire. AMB (ambient control) plots have greenhouse plastic around the plot and buried soil warming cables that are not turned on. +1.5°C and +2.5°C (warming) plots have greenhouse plastic around the plot and buried soil warming cables are set to corresponding temperatures. Information are from Dr. Mohan's team at UGA. For this study, we did not look at canopy effects, which can be a future direction.

Plot	Temperature	Canopy
1	+1.5°C	Gap
2	+2.5°C	Gap
3	AMB	Gap
4	AMB	Gap
5	+1.5°C	Gap
6	+2.5°C	Gap
7	AMB	Gap
8	+2.5°C	Gap
9	+1.5°C	Gap
10	AMB	Forest
11	+1.5°C	Forest
12	AMB	Forest
13	+2.5°C	Forest
14	+1.5°C	Forest
15	+2.5°C	Forest
16	+1.5°C	Forest
17	AMB	Forest
18	+2.5°C	Forest
19	NCC	Gap
20	NCC	Gap
21	NCC	Gap
22	NCC	Forest
23	NCC	Forest
24	NCC	Forest

Table 6: Detailed information about lab equipment used in this study.

Analysis	Equipment Name	Manufacturer	Manufacturer City, State, Country
General Lab Use	Kimtech Purple Nitrile Powder-Free Exam Gloves	Kimberly-Clark Global Sales	Roswell, GA, USA
	Millex Syringe-driven Filter Unit	Merck Millipore Ltd.	Carrigteohill, Co. Cork Ireland
	Disposable Syringe Without Needle	Air-Tie Products Co., Inc.	Virginia Beach, VA, USA
	Whatman No.1 Filter Paper	Cytiva	Germany
	Eppendorf safe-lock tubes	USA Scientific Inc.	Ocala, Florida, USA
CO <sub>2</sub> Mineralization	Qubit System (Q-S151 CO <sub>2</sub> Analyzer)	Qubit Systems Inc.	Kingston, ON, CANADA
Soil Organic C	8000M Mixer Mill	SPEX SamplePrep LLC.	Metuchen, NJ, USA
	ThermoFisher Scientific Elemental Analyzer	ThermoFisher Scientific Inc.	Waltham, MA, USA
Physical (density and size) Fractionation	Sorvall ST Plus Series Centrifuge	ThermoFisher Scientific Inc.	Waltham, MA, USA
	Qsonica Sonicator Ultrasonic Processor	Qsonica, LLC.	Newtown, CT, USA
Microbial Biomass C	Shimadzu TOC-L analyzer	Shimadzu Corporation	Suzhou, Jiangsu, China
Microbial Necromass	Fisherbrand Isotemp Tube Hotplate	ThermoFisher Scientific Inc.	Waltham, MA, USA
Enzyme Activity & Kinetic	Infinite M Nano+ Model: Infinite 200 pro	Tecan Austria	Grodig, Austria